

AD-A054 320

BATTELLE COLUMBUS LABS OHIO
THE ROLE OF TEMPERATURE IN EHD. (U)

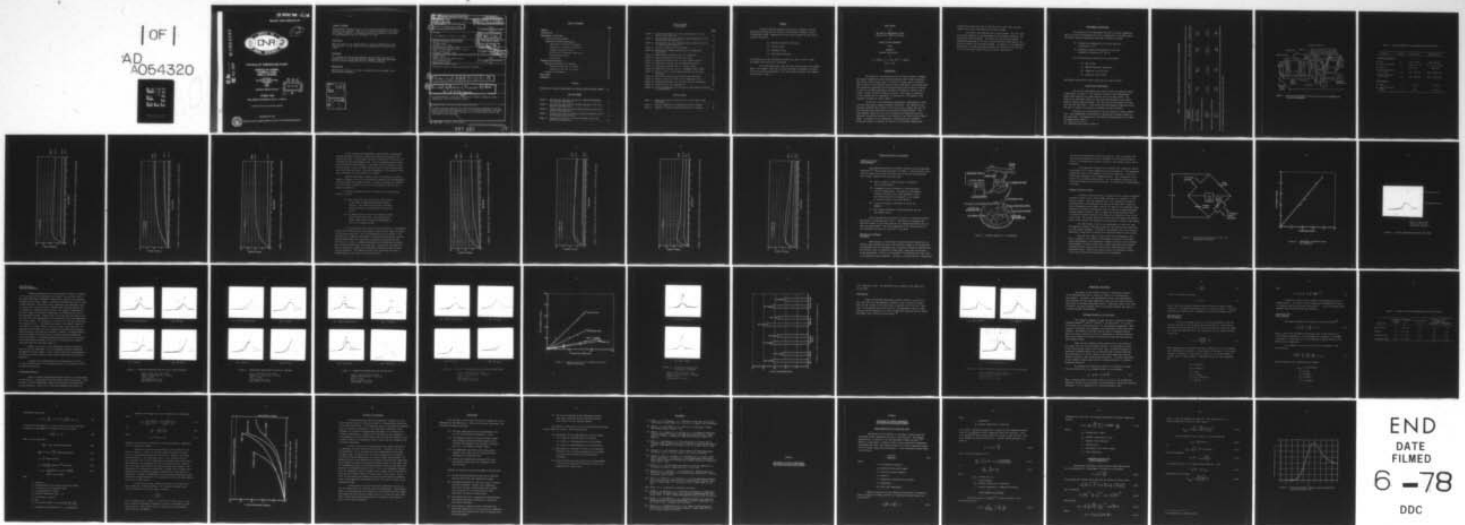
F/G 11/8

UNCLASSIFIED

MAY 78 J W KANNEL, T A DOW, F A ZUGARO
BATT-6-6306

N00014-76-C-0215
ONR-CR229-018-2F NL

| OF |
AD
A054320
MAY 78



END
DATE
FILMED
6-78
DDC

FOR FURTHER TRAN 

REPORT ONR-CR229-018-2F

See A033930

12

AD A 054320



AD No. _____
IDC FILE COPY

THE ROLE OF TEMPERATURE IN EHD

**JERROLD W. KANNEL
THOMAS A. DOW
FRED A. ZUGARO**

**BATTELLE
COLUMBUS LABORATORIES
COLUMBUS
OHIO
43201**

CONTRACT N00014-76-C-0215

DDC
RECEIVED
MAY 26 1978
REGISTERED
E

10 MAY 1978

FINAL REPORT FOR PERIOD 1 OCT 75 - 31 DEC 77

Approved for public release; distribution unlimited.

PREPARED FOR THE



OFFICE OF NAVAL RESEARCH ● 800 N. QUINCY ST. ● ARLINGTON ● VA ● 22217

Change of Address

Organizations receiving reports on the initial distribution list should confirm correct address. This list is located at the end of the report. Any change of address or distribution should be conveyed to the Office of Naval Research, Code 211, Arlington, VA 22217.

Disposition

When this report is no longer needed, it may be transmitted to other organizations. Do not return it to the originator or the monitoring office.

Disclaimer

The findings and conclusions contained in this report are not to be construed as an official Department of Defense or Military Department position unless so designated by other official documents.

Reproduction

Reproduction in whole or in part is permitted for any purpose of the United States Government.

ACCESSION for		
NTIS	White Section	<input checked="" type="checkbox"/>
DCC	Buff Section	<input type="checkbox"/>
UNANNOUNCED		<input type="checkbox"/>
JUSTIFICATION.....		
.....		
BY.....		
DISTRIBUTION/AVAILABILITY CODES		
Dist.	AVAIL. and/or	SPECIAL
A		

18 19 REPORT DOCUMENTATION PAGE		READ INSTRUCTIONS BEFORE COMPLETING FORM	
1. AUTHOR NUMBER ONR-CR229-018-2F	2. GOVT ACCESSION NO.	3. REPORT NUMBER BATT-G-6306	4. TYPE OF REPORT & PERIOD COVERED Final
4. TITLE (and Subtitle) 61 The Role of Temperature in EHD.		5. PERFORMING ORG. REPORT NUMBER G-6306	6. CONTRACT OR GRANT NUMBER(s) 15 N00014-76-C-0215
7. AUTHOR(s) J. W. Kannel, T. A. Dow, F. F. Zugaro	9. PERFORMING ORGANIZATION NAME AND ADDRESS Battelle's Columbus Laboratories 505 King Avenue Columbus, Ohio 43201	10. PROGRAM ELEMENT, PROJECT, TASK AREA & WORK UNIT NUMBERS 11 N.A. 20 May 78	12. REPORT DATE 5/10/78
11. CONTROLLING OFFICE NAME AND ADDRESS Office of Naval Research, Dept. of Navy 800 N. Quincy Street Arlington, Virginia 22217	14. MONITORING AGENCY NAME & ADDRESS (if different from Controlling Office) DCASMA, Dayton Defense Electronics Supply Center 1502 Wilmington Pike Dayton, Ohio 45444	13. NUMBER OF PAGES 56	15. SECURITY CLASS. (of this report) 12 53 p None
16. DISTRIBUTION STATEMENT (of this Report) Approved for public release; distribution unlimited.		15a. DOWNGRADING SCHEDULE N.A.	
17. DISTRIBUTION STATEMENT (of abstracts entered in DIABASE, if different from Report) 9 Final Rept. 1 Oct 75-31 Dec 77,			
18. SUPPLEMENTARY NOTES 10 Jerrold W./Kannel, Thomas A./Dow Fred A./Zugaro			
Elastohydrodynamic, Temperature Transducer, Pressure Transducer, Contact Temperature, Traction, Rolling Contact			
20. ABSTRACT (Continue on reverse side if necessary and identify by block number) A special bisignal transducer has been developed which measures the contact pressure and temperature between a pair of rolling contact disks. Data have been recorded for four common lubricants for different loads, speeds, and conditions of disk sliding.			

407 080

elt

TABLE OF CONTENTS

	<u>Page</u>
SUMMARY.	1
INTRODUCTION	1
EXPERIMENTAL EVALUATIONS	3
Traction-Slip Experiments	3
Temperature-Pressure Experiments.	15
Production of Thin-Film Transducer	15
Calibration of Bisignal Transducer	15
Bisignal Transducer Output	17
Slip Effects on Measured Temperature	21
Rolling Speed Effects.	21
Load Effects	29
THEORETICAL EVALUATIONS.	31
Rheology Evaluations for Tractions.	31
Temperature Rise Due to Sliding.	32
Temperature Ruse Due to Rolling.	33
Critique of Techniques.	38
CONCLUSIONS.	39
REFERENCES	41

APPENDIX

ESTIMATION OF SURFACE TEMPERATURE RISE DURING ROLLING/SLIDING CONTACT.	A-1
--	-----

LIST OF FIGURES

Figure 1. Rolling Disk Apparatus, Set-Up for X-Ray Film Thickness and Traction Measurements	5
Figure 2. Traction-Slip Data for MIL-L-23699 Lubricant at 50 C for Various Load Conditions	7
Figure 3. Traction-Slip Data for MIL-L-23699 Lubricant at 65 C for Various Load Conditions	8
Figure 4. Traction-Slip Data for Synthetic Mineral Lubricant at 50 C for Various Load Conditions	9
Figure 5. Traction-Slip Data for Traction Lubricant at 50 C for Various Load Conditions	11

LIST OF FIGURES
(Continued)

	<u>Page</u>
Figure 6. Traction-Slip Data for Traction Lubricant at 65 C for Various Load Conditions	12
Figure 7. Traction-Slip Data for Polyphenyl Ether Lubricant at 50 C for Various Load Conditions	13
Figure 8. Traction-Slip Data for Polyphenyl Ether Lubricant at 65 C for Various Load Conditions	14
Figure 9. Pictorial Drawing of P-T Transducer	16
Figure 10. Self Pressure-Compensating Circuit for Temperature Experiments	18
Figure 11. Temperature Calibration Curve for Thermistor.	19
Figure 12. Typical Temperature-Pressure Scope Trace	20
Figure 13. Temperature-Pressure Data for MIL-L-23699 Lubricant	22
Figure 14. Temperature Pressure Data for XRM-109 Lubricant	23
Figure 15. Temperature Pressure Data for Traction Fluid.	24
Figure 16. Temperature Pressure Data for Polyphenyl Ether (5P4E)	25
Figure 17. Effect of Slip on Exit Temperature Rise for Selected Lubricants	26
Figure 18. Temperature Pressure Data for Selected Lubricants	27
Figure 19. Effect of Speed on "Pure" Rolling Temperature Rise.	28
Figure 20. Temperature-Pressure Data for Four Selected Lubricants.	30
Figure 21. Predicted Inlet Zone Temperature.	37
Figure A-1. Surface-Temperature Function Versus Dimensionless Position in Contact Zone.	A-5

LIST OF TABLES

Table 1. Approximate Lubricant Properties for Fluids Used in BCL Experiments	4
Table 2. Typical Parameters for Temperature-Traction Studies	6
Table 3. Estimate of Surface Temperature Rise Due to Sliding	34

SUMMARY

A special bisignal (pressure-temperature) transducer has been developed which measures the contact zone temperature between a pair of rolling steel disks. Temperature data have been recorded for the following four lubricants:

- (1) Synthetic paraffinic lubricant
- (2) Traction fluid
- (3) Polyphenyl ether
- (4) MIL-L-23699 lubricant.

The conditions for the experiments include two loads (.7 and 1.1 GPa), two speeds, and several slip conditions.

Very large temperature rises have been seen in many of the experiments. For example, under pure rolling conditions, temperature in excess of 30 C rise have been measured. For high sliding conditions, the temperature may rise to 200 C.

FINAL REPORT

on

THE ROLE OF TEMPERATURE IN EHD
(Contract No. N00014-76-C-0215)

to

OFFICE OF NAVAL RESEARCH

from

BATTELLE

Columbus Laboratories

by

J. W. Kannel, T. A. Dow, and F. F. Zugaro

May 9, 1978

INTRODUCTION

The purpose of the research project has been to measure, evaluate, and analyze temperatures under elastohydrodynamic (EHD) contact conditions. EHD contact occurs in many types of rolling or sliding contact situations, such as roller or ball-bearing contacts, gear tooth meshes, and rolling disks. The temperature measurement technique developed during the project involves the use of a titanium temperature transducer (thermistor) coated on one of a pair of disks rolling in lubricated contact. The change in resistance of the titanium, due to temperature, is detected for each passage of the transducer through the contact region.

In addition to the temperature measurements, measurements of pressure were made using a manganin pressure transducer. The temperature and pressure transducer were located on the disk in such a manner that the contact pressures and temperatures could be detected simultaneously. With this bisignal system, not only can the pressure and temperature level be detected, but also the location of one relative to the other could be determined. In addition to the experiments, analyses have been performed during the project to estimate the sources of the measured temperatures.

Considerations have been given to effects such as inlet shear heating, compressive heating, and heating due to disk slippage.

The project was conducted over a 2-year period. The first year was devoted primarily to the development of the bisignal transducer and preliminary thermal analyses. The second year has involved numerous temperature measurements for four selected lubricants under several conditions of speed, load, and disk slippage. In addition to the temperature measurements, traction measurements under slip conditions have been made to aid in analyzing thermal effects on contact temperatures.

EXPERIMENTAL EVALUATIONS

The objective of the experiments has been to develop fundamental data to be used for determining the role of temperature in the EHD process. Two general types of experiments have been conducted as follows:

- (1) Traction-slip experiments on the type described in Reference (1)^(a)
- (2) Temperature-pressure measurements of the type described in References (2) and (3)

Four lubricants were selected for the experiments:

- (1) MIL-L-23699
- (2) XRM-109 (Synthetic Paraffinic)
- (3) Commercial traction fluid
- (4) Polyphenyl ether (5P4E) .

Approximate properties for these lubricants are given in Table 1.

Traction-Slip Experiments

The traction experiments were conducted using the apparatus shown schematically in Figure 1. The apparatus consists of two independently-driven disks which can be loaded together into lubricated contact. The disks are on stub-shafts which fit into drive shafts mounted in precision (ABEC-7) angular contact bearings. The rotor for the drive motors are integral with the disk shafts. These motors are high-frequency induction motors, the speed of which can be varied by changing the input frequency.

The disks are jet-lubricated by the test fluid at a preset temperature. Disk temperature is monitored by a thermocouple located outboard of the upper disks. The geometry and load-pressure characteristics of the disk are summarized in Table 2.

(a) References are listed on Page 41.

TABLE 1. APPROXIMATE LUBRICANT PROPERTIES FOR FLUIDS USED IN BCL EXPERIMENTS

Lubricant/ Parameter	MIL-L-23699 (a)	Synthetic Mineral Oil	Traction Fluid	Polyphenyl Ether
Base Viscosity				
(Cp at 38 C)	26.9	369.0	29.87	341.8
(Cp at 100 C)	4.9	29.8	4.80	12.7
Base Pressure Viscosity Coefficient				
(GPa) ⁻¹	12.7 x 10 ⁻⁴	19.9 x 10 ⁻⁴	19.9 x 10 ⁻⁴	42.6 x 10 ⁻⁴
(Psi) ⁻¹	.9 x 10 ⁻⁴	1.4 x 10 ⁻⁴	1.4 x 10 ⁻⁴	3 x 10 ⁻⁴
Temperature Viscosity Coefficient				
(F) ⁻¹	.016	.023	.016	.029
(C) ⁻¹	.029	.041	.029	.052

(a) Furnished by Wright-Patterson Air Force Base (ATL-7015).

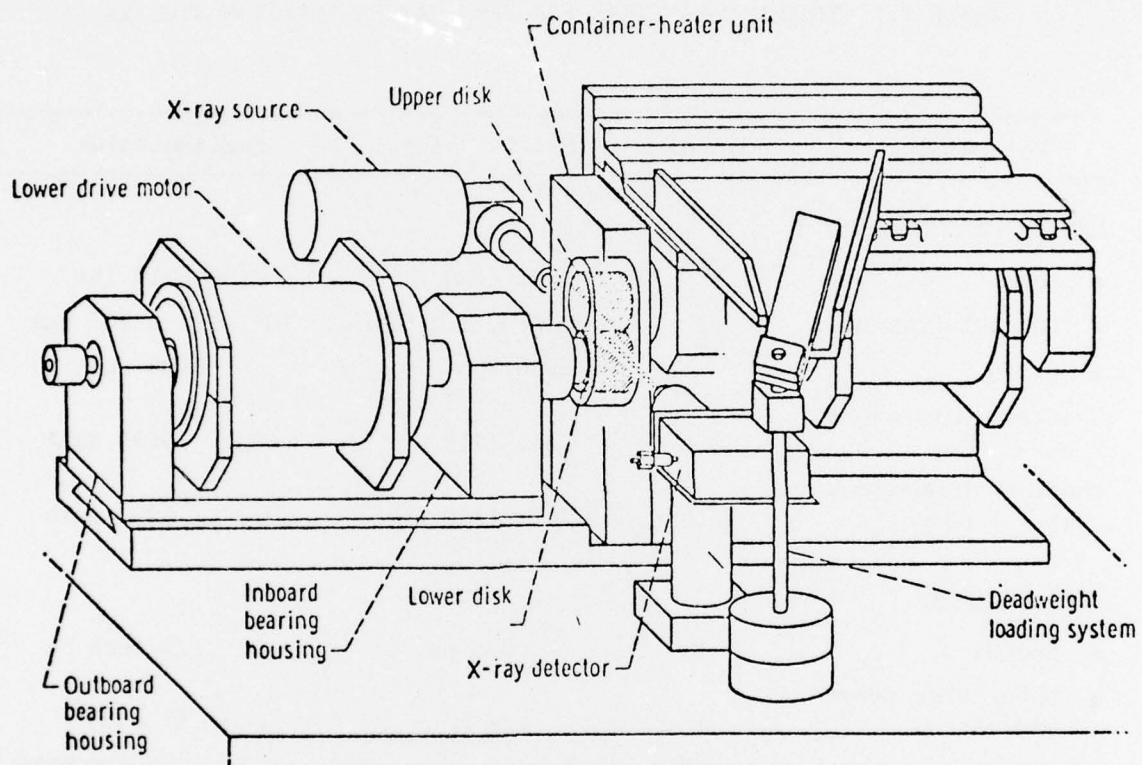


FIGURE 1. ROLLING DISK APPARATUS, SET-UP FOR X-RAY FILM THICKNESS AND TRACTION MEASUREMENTS

TABLE 2. TYPICAL PARAMETERS FOR TEMPERATURE-TRACTION STUDIES

Parameter	Symbol	Metric Value	English Value
<u>Operating Condition</u>			
● Load	W	450, 1400 N	100, 315 lbs
● Contact Pressure	p_H	.7 GPa, 1.1 GPa	10^5 , 1.5×10^5 psi
● Speed		2900 rpm	2900 rpm
Contract Dimensions at .7 GPa	a,b	233, 1259 μm	.0091, .0491 inch
Contract Dimensions at 1.1 GPa	a,b	351, 1890 μm	.0137, .0737 inch
<u>Disk Geometry</u>			
● Radius	R	.038 μm	1.5 inch
● Upper Disk Crown Radius	R	.28 m	11 inch

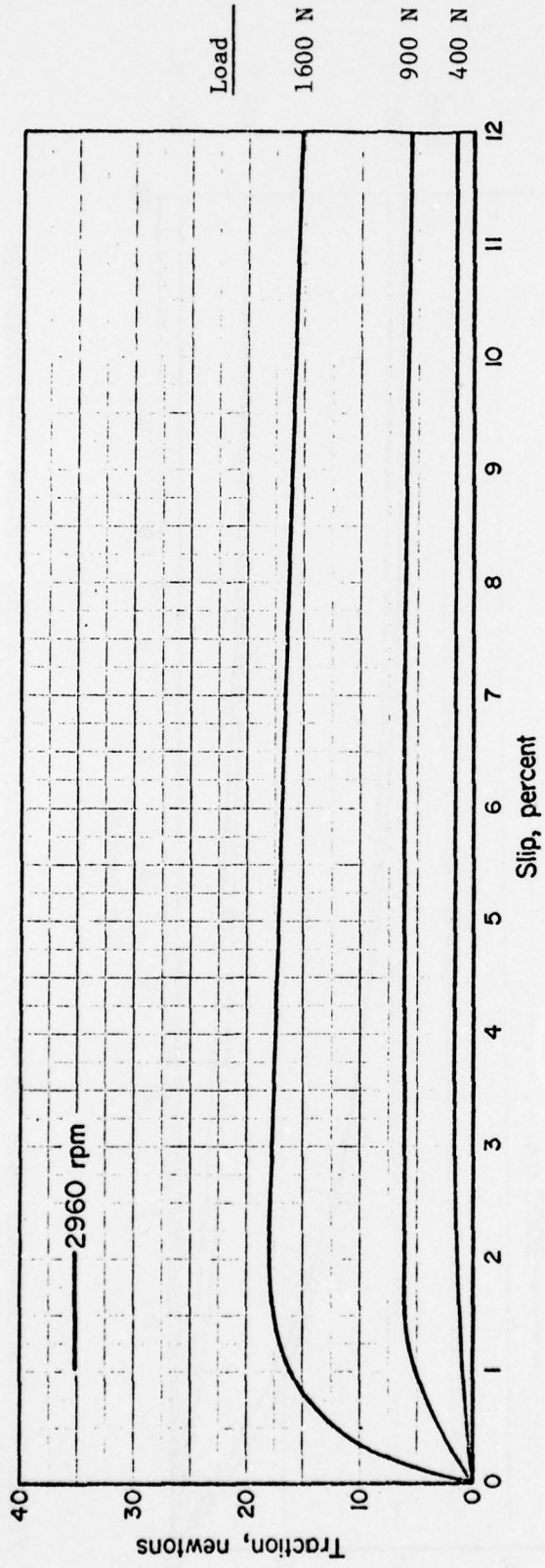


FIGURE 2. TRACTION-SLIP DATA FOR MIL-L-23699 LUBRICANT AT 50 C FOR VARIOUS LOAD CONDITIONS

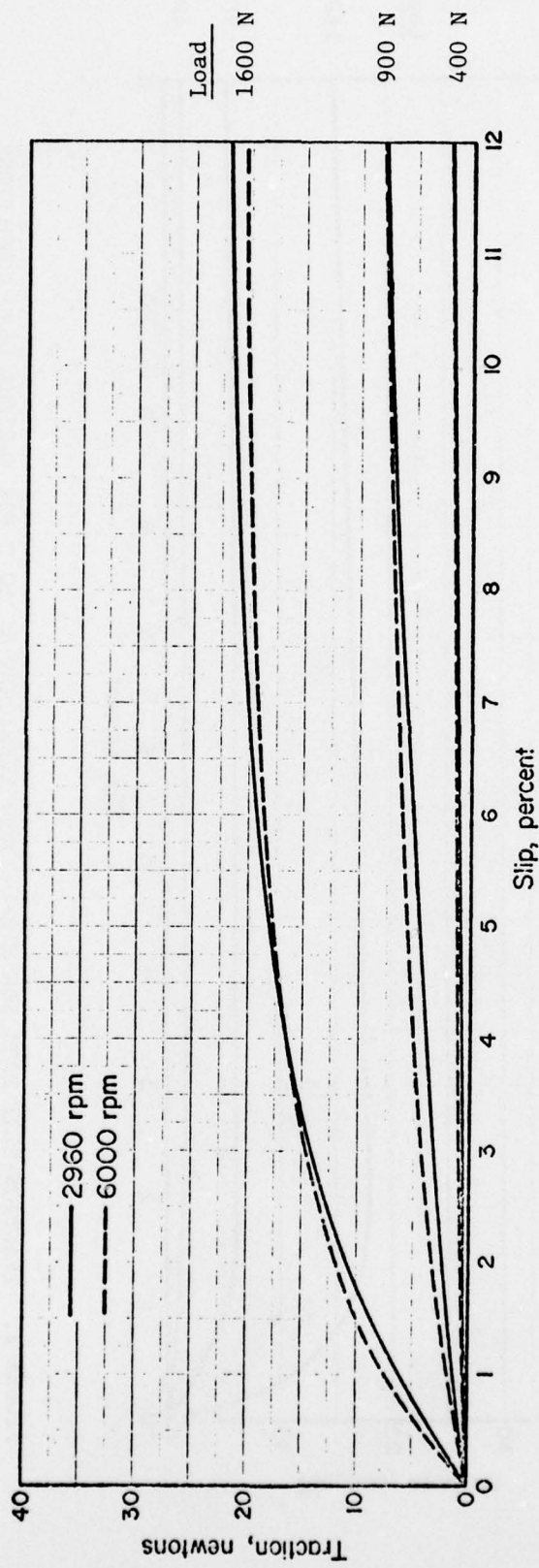


FIGURE 3. TRACTION-SLIP DATA FOR MIL-L-23699 LUBRICANT AT 65 C FOR VARIOUS LOAD CONDITIONS

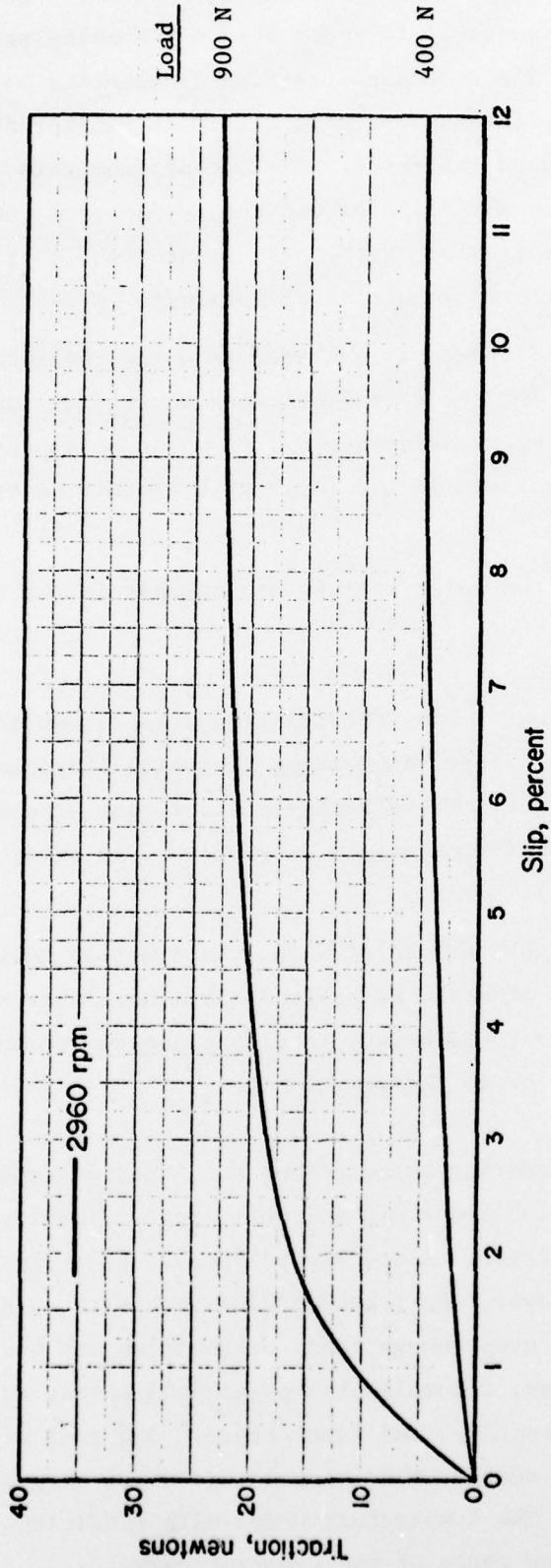


FIGURE 4. TRACTION-SLIP DATA FOR SYNTHETIC MINERAL LUBRICANT AT 50 C FOR VARIOUS LOAD CONDITIONS

In the traction slip experiments, disk slippage is achieved by reducing the input frequency to upper disk drive motor relative to the lower drive motor. The attendant traction is detected by a load cell constraining the upper-disk support unit. Slip is monitored using a differential electronic speed indicator. The output from this indicator is fed into the x-axis of an x-y recorder and the output from the traction-load cell is fed into the y-axis. With this arrangement, a traction-slip curve can be generated for each condition of interest.

Traction slip data as extracted from x-y recordings are given in Figures 2 through 8 for the four lubricants at several load and temperature conditions using 76 mm diameter disks. As would be expected, an increase in load yields an increase in the level of the measured traction for a given slip condition.

There are two major regions of interest in the traction slip curves as follows:

- (1) Near zero slip, the traction slip curves appear to be linear, suggesting Newtonian lubricant behavior. For a Newtonian lubricant, the shear stress (traction) is proportional to shear rate (slip).
- (2) At higher values of slip, the traction no longer rises linearly with slip. This nonlinear behavior could be due to either non-Newtonian effects or to thermal heating.

It is interesting to note that the traction behavior of the XRM-109 and the MIL-L-23699 lubricant are somewhat similar despite large differences in their base viscosities. Also, the polyphenyl ether is similar to the traction fluid. However, the traction fluid exhibits much greater traction than the MIL-L-23699 even though their viscosities are nearly the same. Traction is, of course, a complicated phenomenon involving EHD film thickness, contact zone rheology, and temperature. One goal of the project has been to evaluate the contact zone temperature under slip as well as pure rolling conditions. The temperature under slip conditions will have a profound impact on the shape of the traction curve.

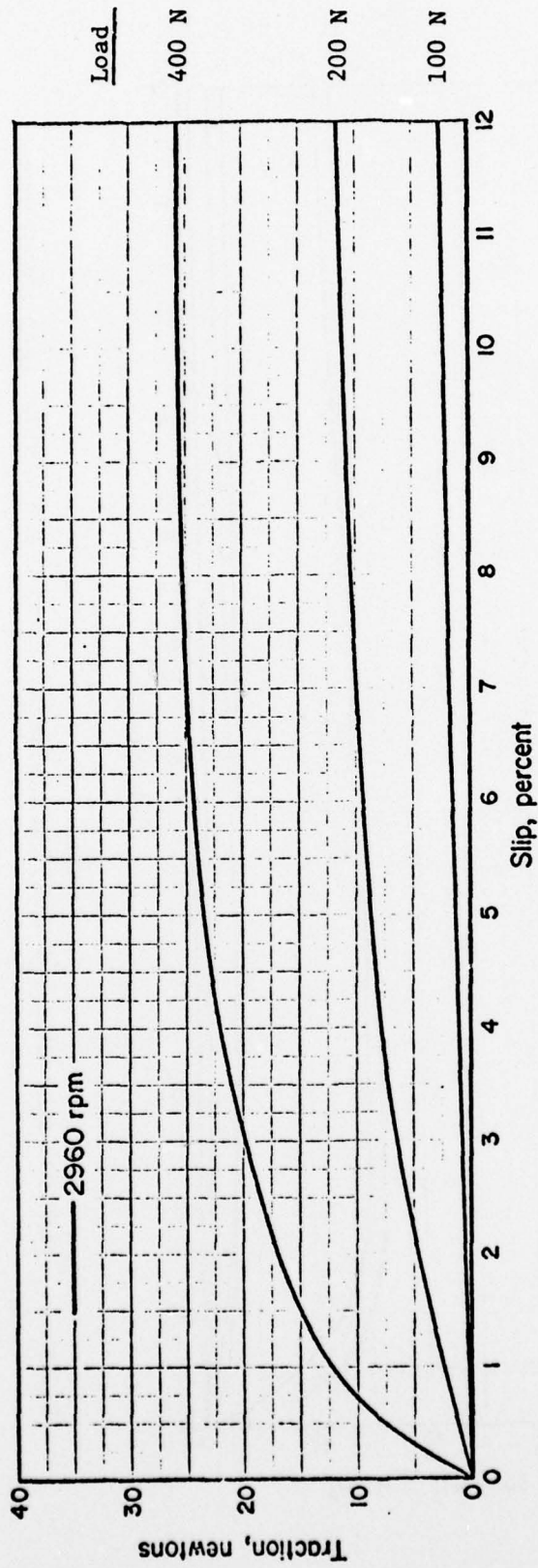


FIGURE 5. TRACTION-SLIP DATA FOR TRACTION LUBRICANT AT 50 C FOR VARIOUS LOAD CONDITIONS

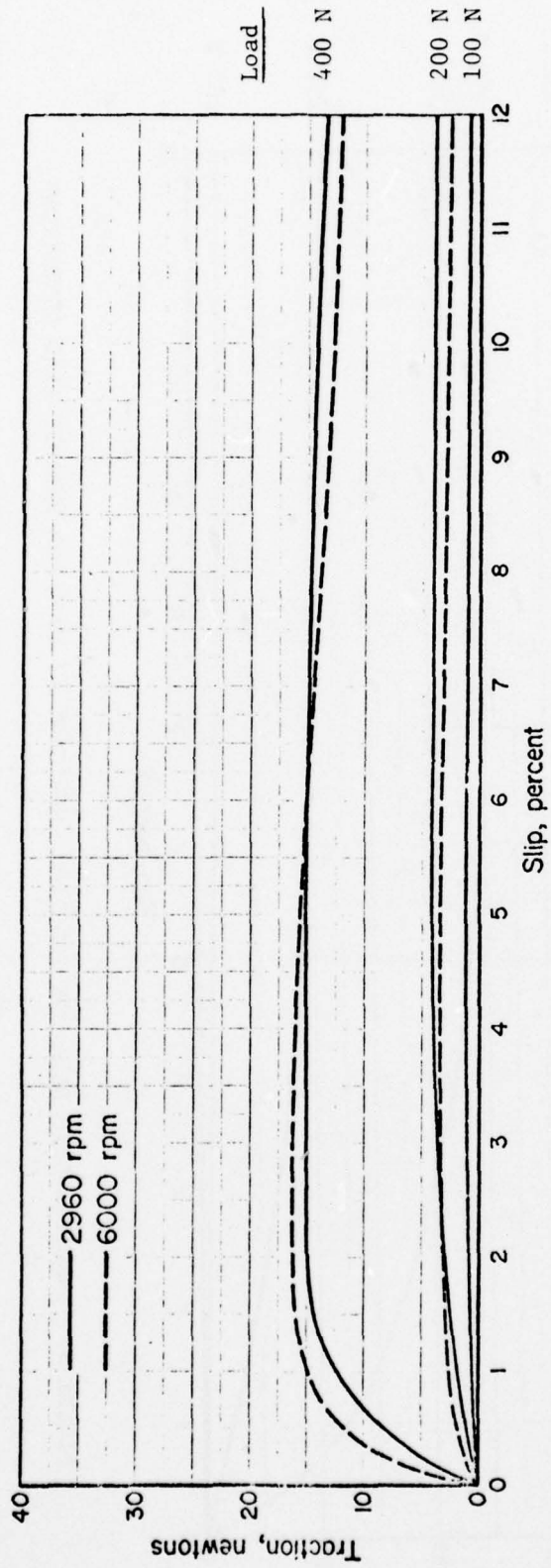


FIGURE 6. TRACTION-SLIP DATA FOR TRACTION LUBRICANT AT 65 C FOR VARIOUS LOAD CONDITIONS

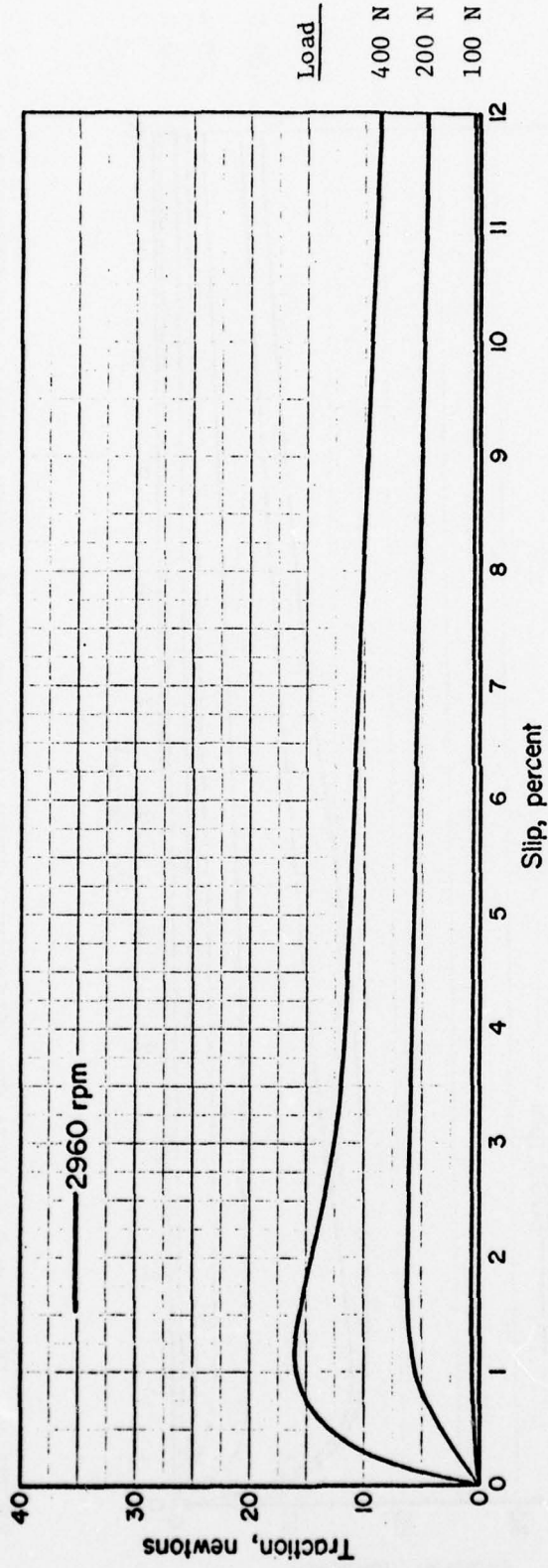


FIGURE 7. TRACTION-SLIP DATA FOR POLYPHENYL ETHER LUBRICANT AT 50 C FOR VARIOUS LOAD CONDITIONS

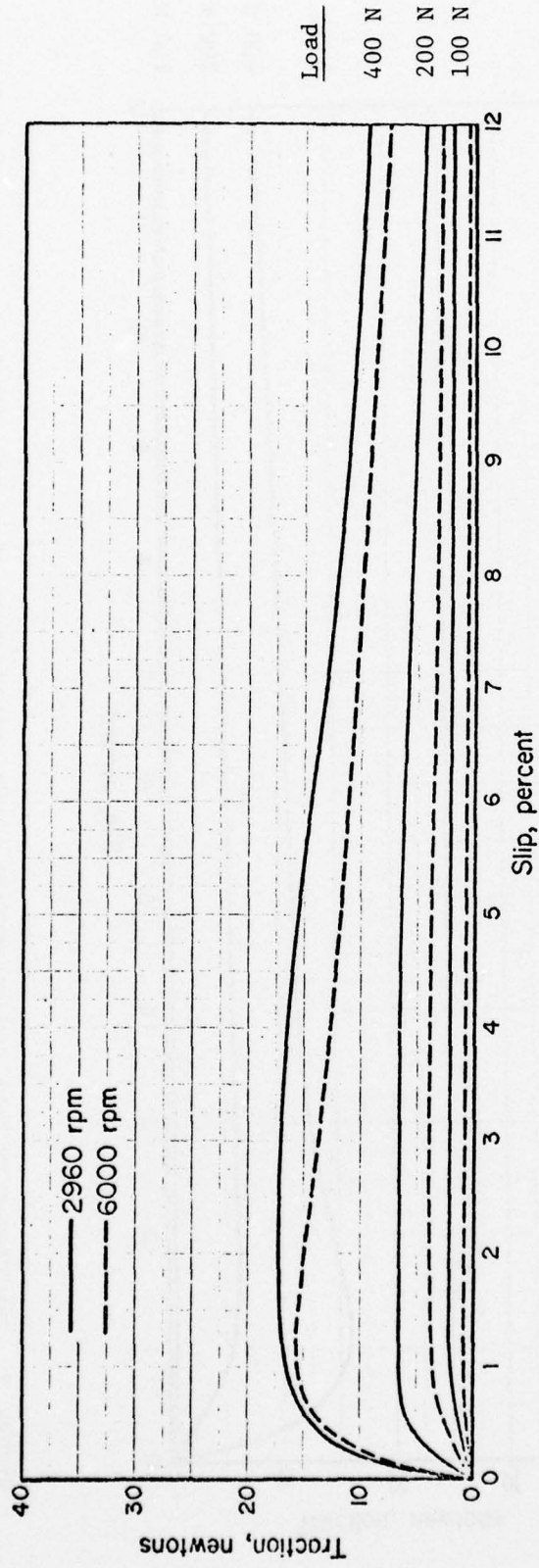


FIGURE 8. TRACTION-SLIP DATA FOR POLYPHENYL ETHER LUBRICANT AT 65 C FOR VARIOUS LOAD CONDITIONS

Temperature-Pressure Experiments

Production of Thin-Film Transducer

The temperature-pressure (bisignal) transducer has been described previously^(2,3) and is shown pictorially in Figure 9. This thin-film transducer is coated directly onto the lower disk of the twin disk apparatus. This process consists of the following steps:

- (1) First, a layer of alumina (Al_2O_3) is sputtered onto the disk surface.
- (2) A manganin pressure transducer is vapor-deposited onto the alumina layer. The shape of this manganin coating (see Figure 9) has been designed to allow the active region of the transducer to be located in the axial center of the disk surface.
- (3) A layer of alumina is sputtered on top of the manganin.
- (4) The titanium thermistor is vapor-deposited onto the last alumina layer.

All of the deposition processes are done in a controlled environment broken only between Steps 2 and 3. The shape of the manganin and titanium coatings is controlled with the aid of masks manipulated from outside the vacuum chamber. The final dimensions of the active portions of the transducers are about 50 x 200 μm by .1 μm thick.

Calibration of Bisignal Transducer

Theoretically, as the bisignal transducer passes through the conjunction region between the disks, the resistance change of the titanium due to temperature and of the manganin due to pressure is detected simultaneously. The circuitry used is a Wheatstone bridge with a high-speed oscilloscope as the galvanometer. However, as discussed⁽³⁾ the thermistor has been found to be somewhat pressure sensitive. Therefore, a special pressure compensating

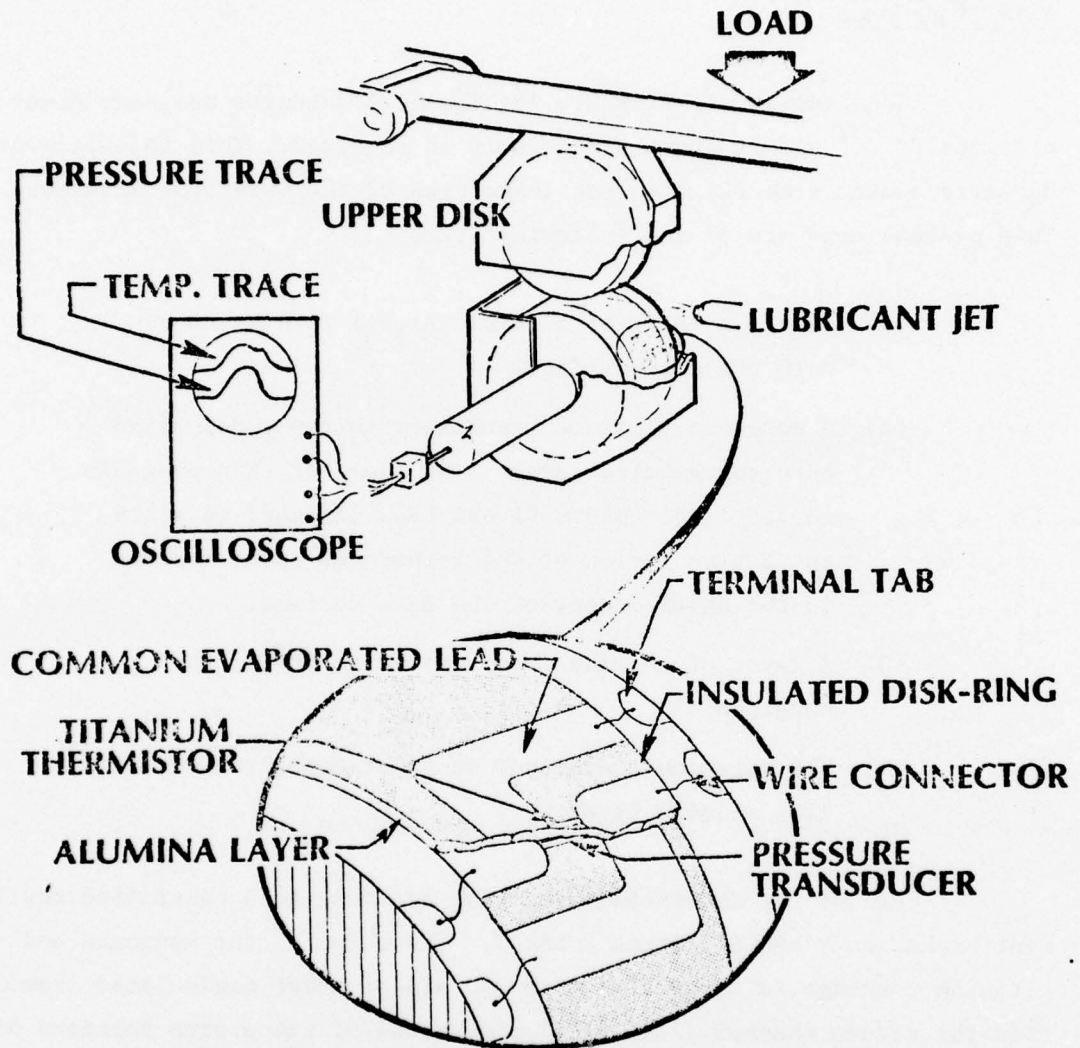


FIGURE 9. PICTORIAL DRAWING OF P-T TRANSDUCER

circuit has been developed as shown in Figure 10. Here, the signal from the pressure transducer is used to compensate for the titanium pressure effects. By adjusting the variable resistors, this pressure effect can be minimized.

The temperature transducer was calibrated for temperature effects by spraying oil at a known temperature onto the thermistor. The temperature calibration curve for the thermistor is given in Figure 11; 1 mv on the oscilloscope represents an 8 C temperature rise. This calibration is consistent with previously reported data. For the pressure calibration, the output was compared with the known loading. The calibration is approximately .18 GPa/mv.

Bisignal Transducer Output

A typical oscilloscope trace, obtained with the bisignal transducer, is given in Figure 12 for a MIL-L-23699 lubricant at a loading of 1.1 GPa contact pressure. Since the compensating circuit (Figure 10) precludes recording pressure and temperature at exactly the same time, a double exposure photograph has been made; that is, an image of the temperature trace immediately followed by the pressure trace is taken on a single photograph. A single magnetic pickup is used to trigger the oscilloscope and, hence, to provide horizontal location of the pressure or temperature trace on the scope screen. The shutter speed of the camera was slow enough that several traces of the pressure and temperature distributions are shown in the figures.

The inlet region in all of the photographs is on the left side. The temperature grows in the inlet region and, for pure rolling, peaks near the peak pressure gradient. The shape of the pressure trace is very near a semielliptic shape which is similar to the Hertzian theory for dry contact.

Near the exit region, a "dip" occurs in the temperature curve. This is thought to be a result of the pressure correction circuit and a slight misalignment of the temperature transducer relative to the pressure. A misalignment of 30-50 μm could cause a small region where the pressure compensation would cease to exist and cause an artificial drop in the temperature trace. Outside the pressure region, the thermistor returns to the proper level since pressure effects are negligible.

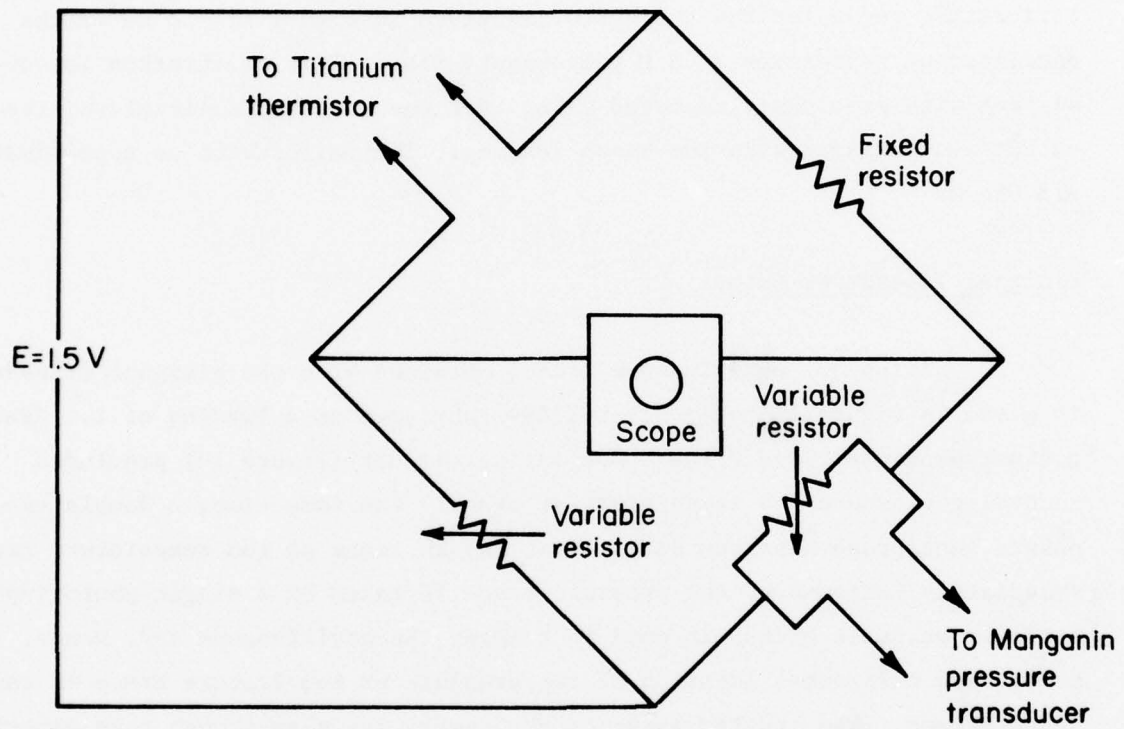


FIGURE 10. SELF PRESSURE-COMPENSATING CIRCUIT FOR TEMPERATURE EXPERIMENTS

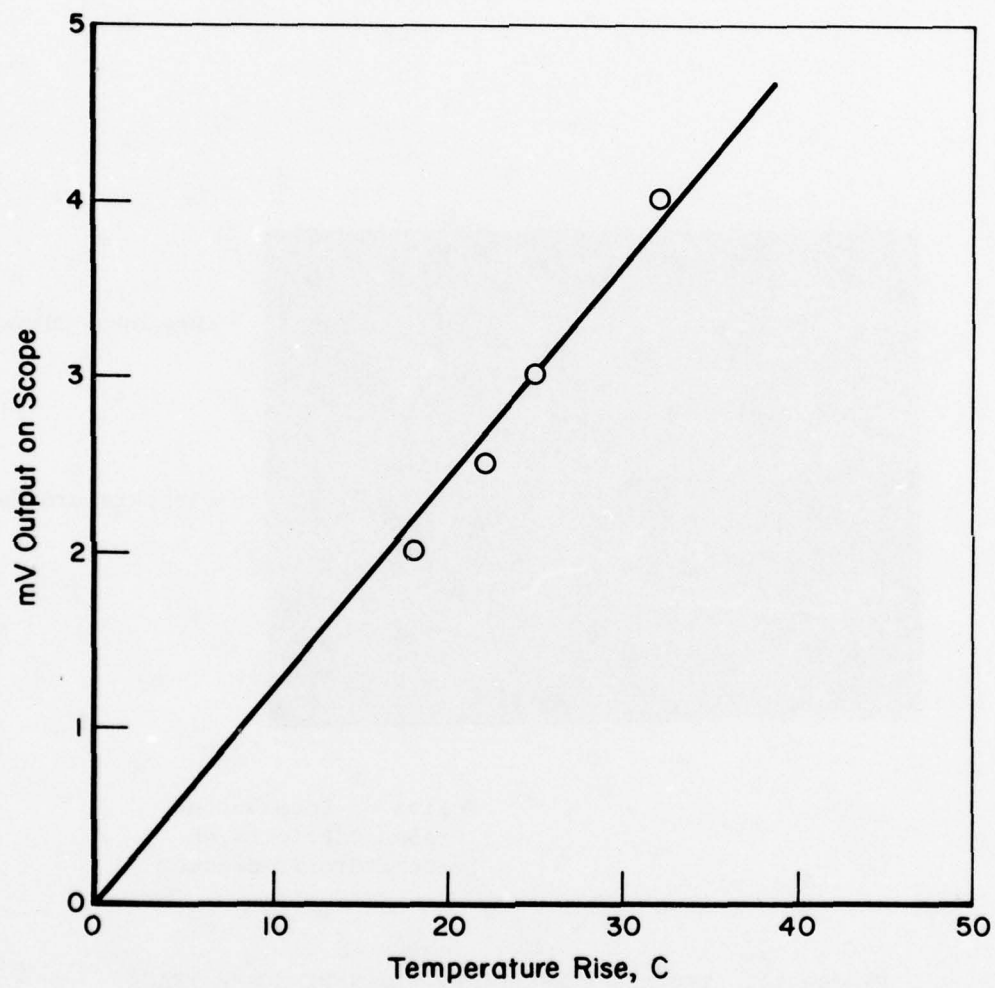


FIGURE 11. TEMPERATURE CALIBRATION CURVE FOR THERMISTOR

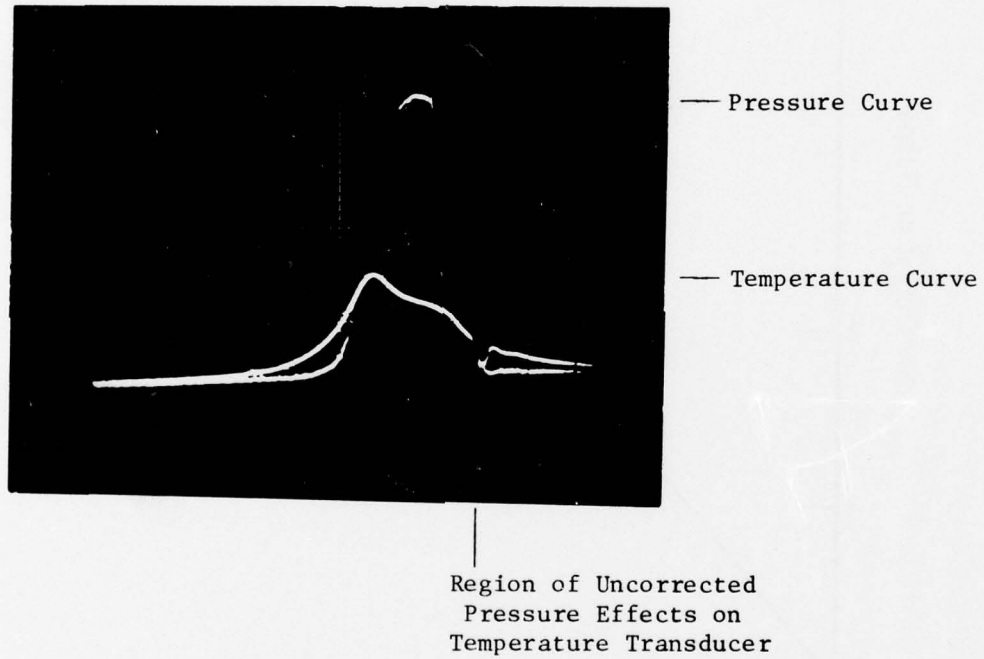


FIGURE 12. TYPICAL TEMPERATURE-PRESSURE SCOPE TRACE

Slip Effects on Measured Temperature

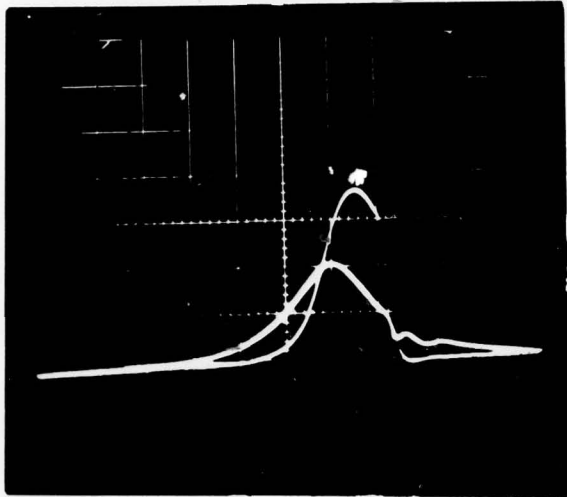
Temperature-pressure traces are presented in Figures 13 through 16 for the four selected lubricants (see Table 1) for one load (400 N), one speed (2800 rpm), and ambient temperature at various slip conditions including pure rolling. Figure 13 presents the temperature data for a MIL-L-23699 lubricant. Under pure rolling conditions, the temperature rises to a peak of 32 C near the point of maximum inlet pressure gradient and is followed by a gradual temperature drop. The growth of temperature in the inlet region is caused by a combination of rolling shear on the oil and compressive heating. Figures 13(b) to (d) show that slip does not affect the inlet zone temperature but does materially effect the temperature at the exit region. For example, at 17 percent slip, the exit temperature has increased by 30 C. The temperature data for the XRM-109 (Figure 14) are similar to the MIL-L-23699. For the traction fluid (Figure 15) and polyphenyl ether (Figure 16), the temperature rise under pure rolling is about the same as the other two lubricants. However, the temperatures do not decay through the contact region for these fluids even under pure rolling conditions. An enormous temperature rise occurs for the traction fluid under high slip [Figure 15(a)] due to the high level of traction associated with this fluid (see Figure 5).

Figure 17 is a plot of exit temperature rise as a function of slip for the four lubricants. As can be observed, the MIL-L-23699 and the XRM-107 are quite similar. Also, it can be seen that the temperature rise with the traction fluid is significantly larger than for the other lubricants.

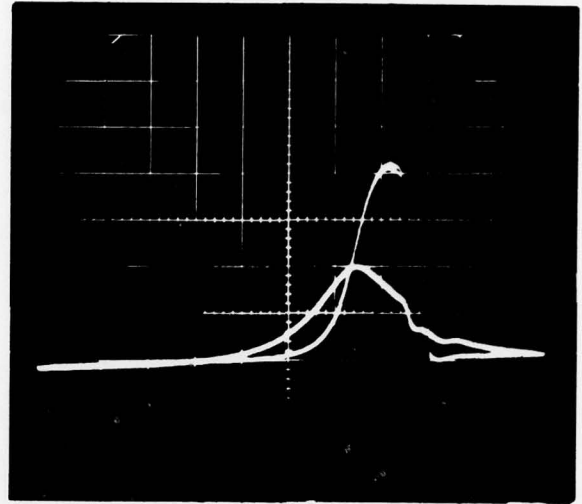
In general, the high magnitude of the temperature rise due to slip could explain much of the nonlinearities seen in traction-slip curves at high slip conditions.

Rolling Speed Effects

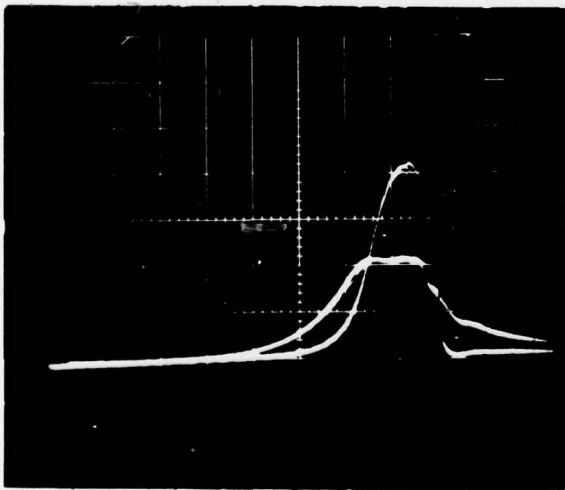
Figure 18 presents temperature-pressure traces for a rolling speed of 1400 rpm (i.e., approximately half the speed of the previous data). This reduction in speed significantly reduced the temperature rise under pure rolling conditions. Figure 19 is a bar graph showing speed effects on



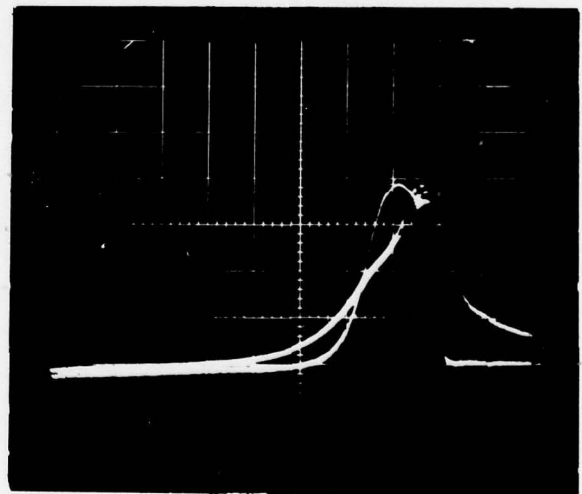
(a) "Pure" Rolling Disk



(b) 4% Slip



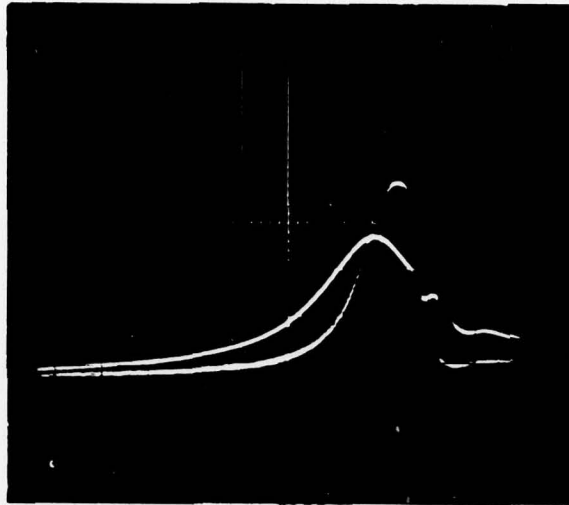
(c) 7% Slip



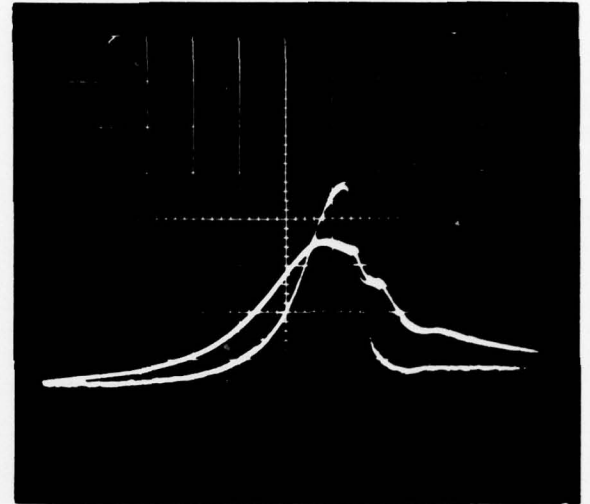
(d) 17% Slip

FIGURE 13. TEMPERATURE-PRESSURE DATA FOR A MIL-L-23699 LUBRICANT

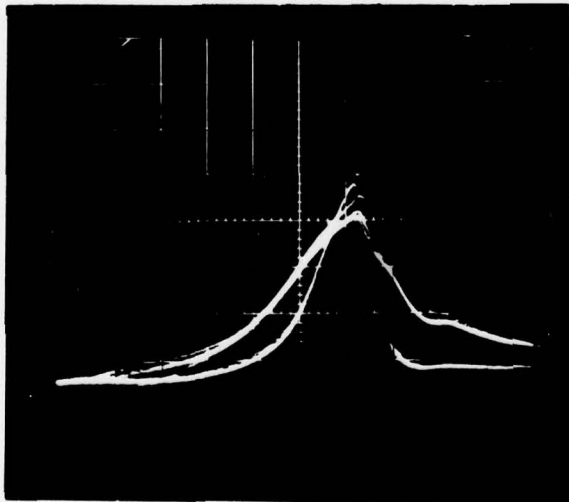
Speed = 2800 rpm (.076 m disk)
 Temperature Calibration = 16 C/div
 Load = .7 GPa
 Oil Temperature = 35 C
 Scope Sweep = 20 μ s/div



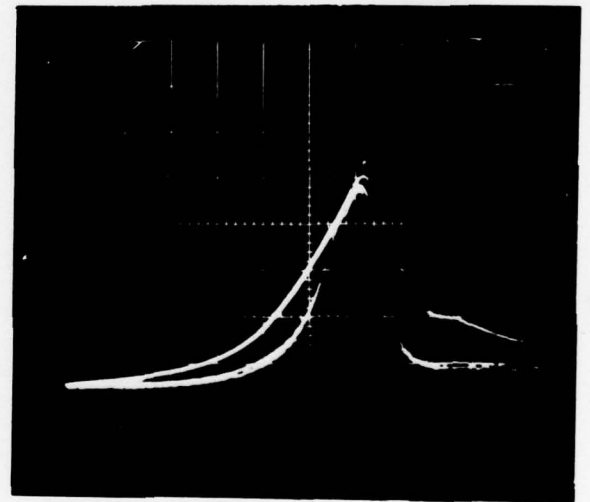
(a) "Pure" Rolling Disk



(b) 7% Slip



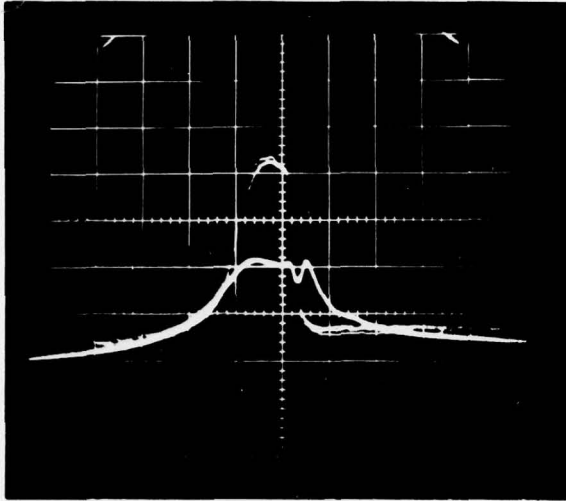
(c) 15% Slip



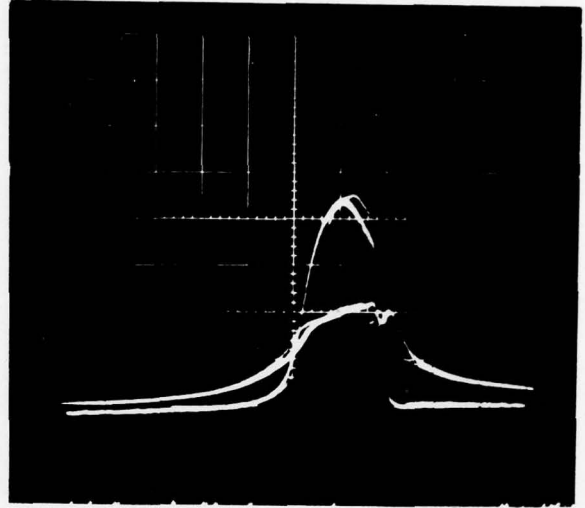
(d) 23% Slip

FIGURE 14. TEMPERATURE PRESSURE DATA FOR XRM-109 LUBRICANT

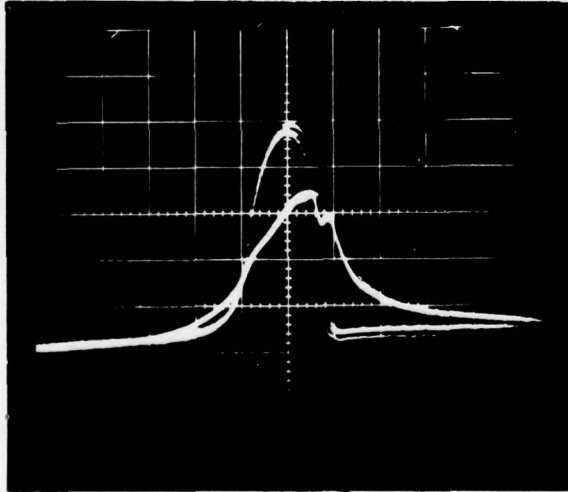
Speed = 2800 rpm (.076 m disk)
 Temperature Calibration = 16 C/div
 Load = .7 GPa
 Oil Temperature \approx 45 C
 Scope Sweep = 20 μ s/div



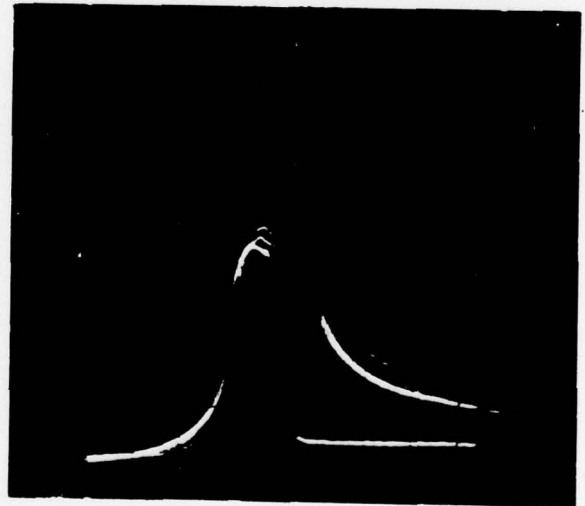
(a) "Pure" Rolling Disk



(b) 1.5% Slip



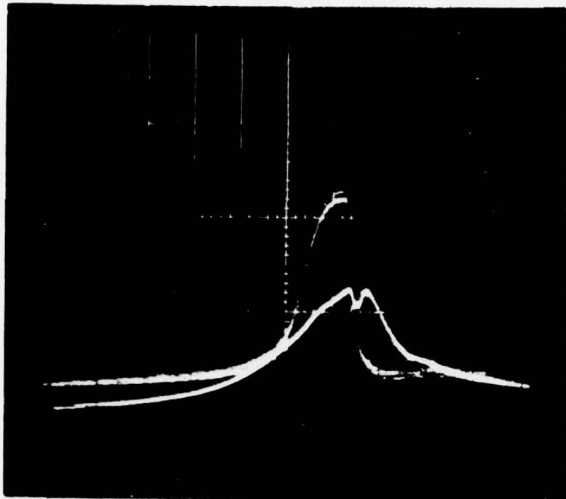
(c) 2.2% Slip



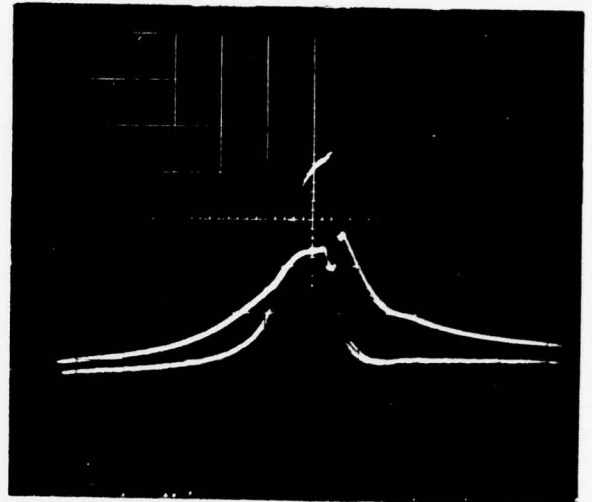
(d) 13% Slip

FIGURE 15. TEMPERATURE PRESSURE DATA FOR TRACTION FLUID

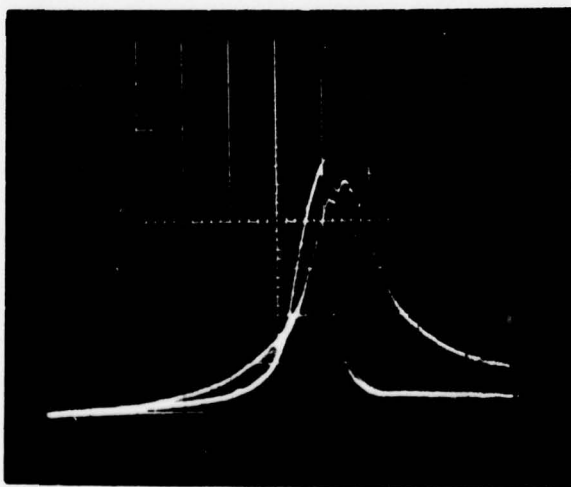
Speed = 2000 rpm (.076 m disk)
 Temperature Calibration = 16 C/div
 Load = .7 GPa
 Oil Temperature \approx 35 C
 Scope Sweep = 20 μ s/div



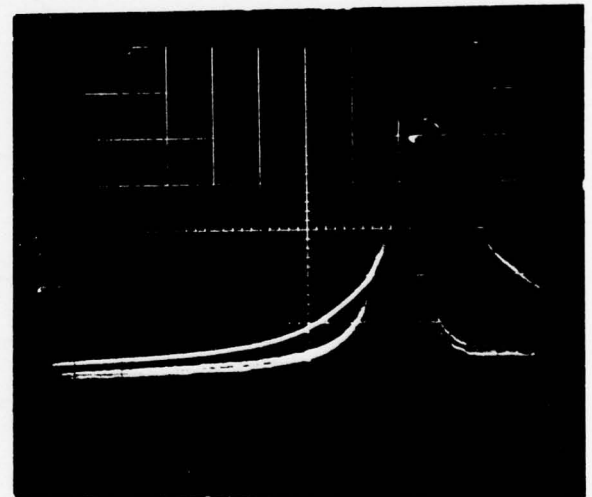
(a) "Pure" Rolling Disk



(b) 2.5% Slip



(c) 10% Slip



(d) 13% Slip

FIGURE 16. TEMPERATURE PRESSURE DATA FOR POLYPHENYL ETHER (5P4E)

Speed = 2800 rpm (.076 m disk)
 Temperature Calibration = 16 C/div
 Load = .7 GPa
 Oil Temperature \approx 45 C
 Scope Sweep = 20 μ s/div

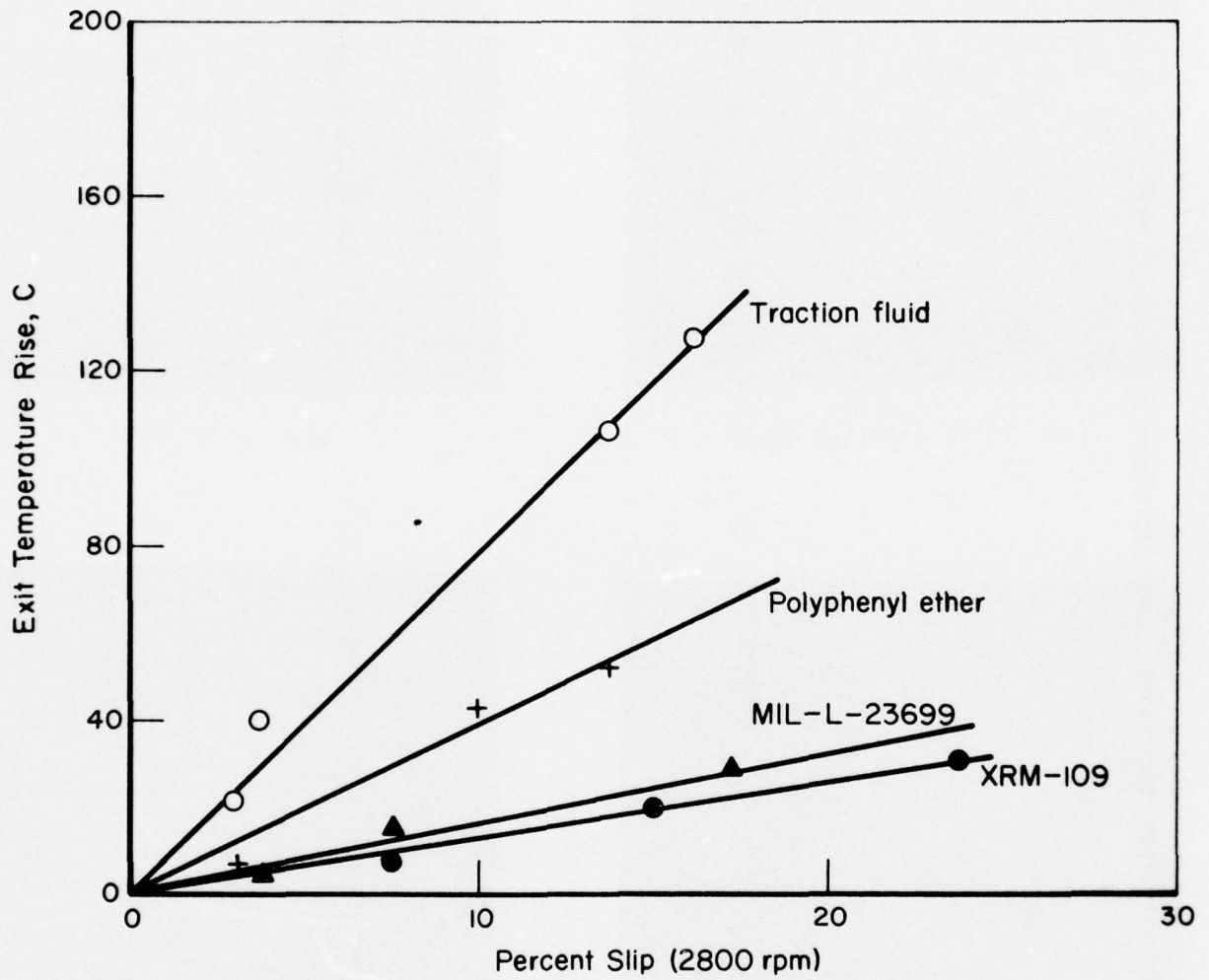
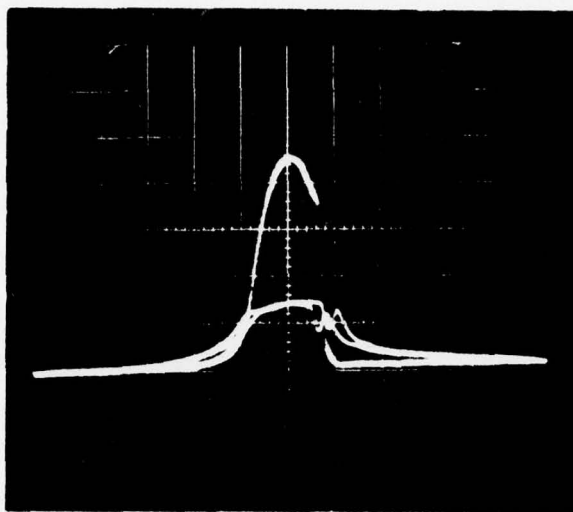
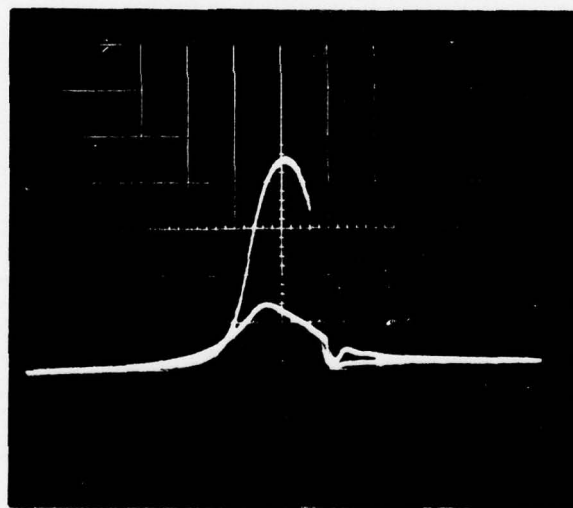


FIGURE 17. EFFECT OF SLIP ON EXIT TEMPERATURE RISE FOR SELECTED LUBRICANTS



(a) Traction Fluid



(b) MIL-L-23699

FIGURE 18. TEMPERATURE PRESSURE DATA
FOR SELECTED LUBRICANTS

Speed = 1400 rpm (.076 m disk)
Temperature Calibration = 16 C/div
Load = .7 GPa
Scope Sweep = 40 μ s/div

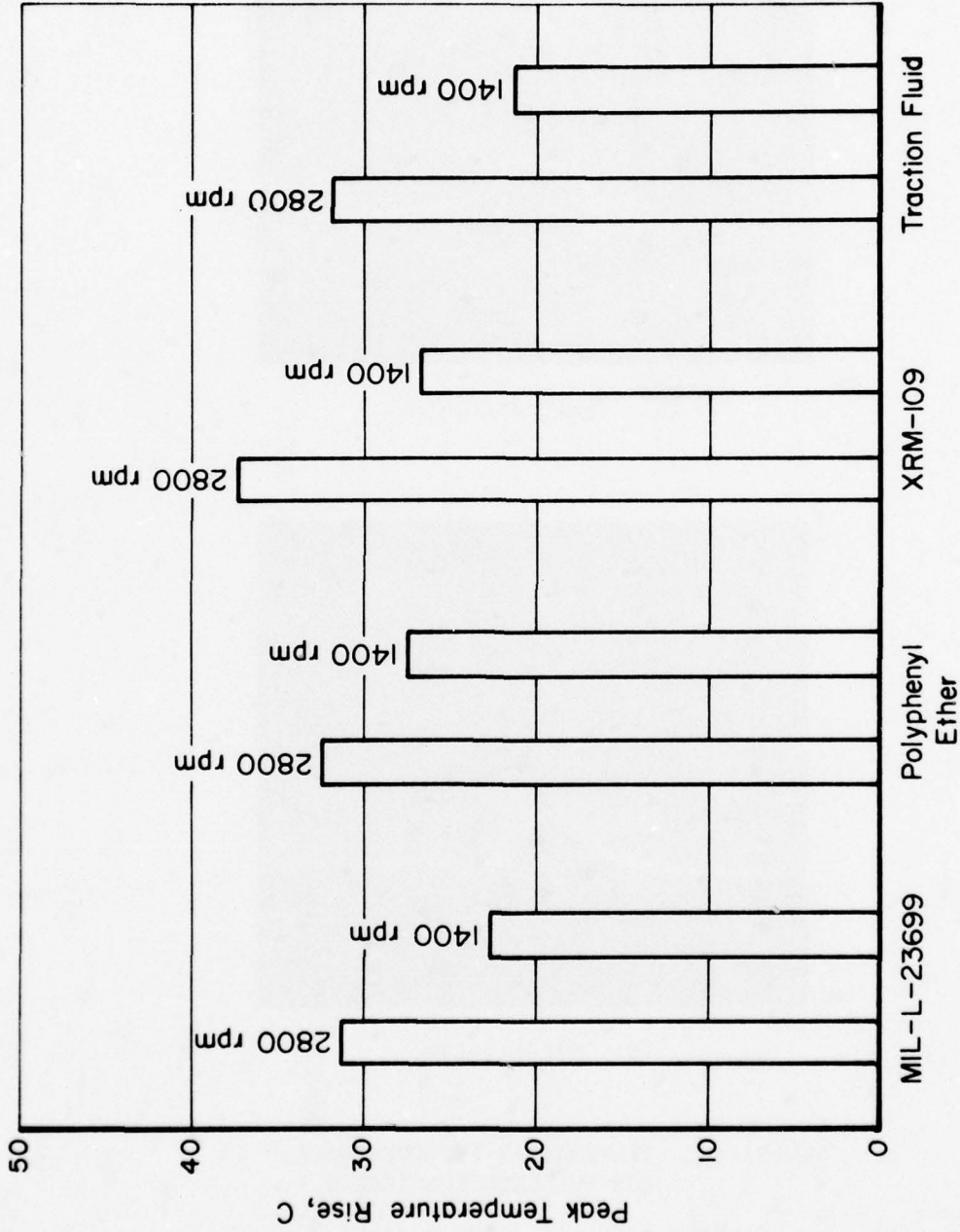
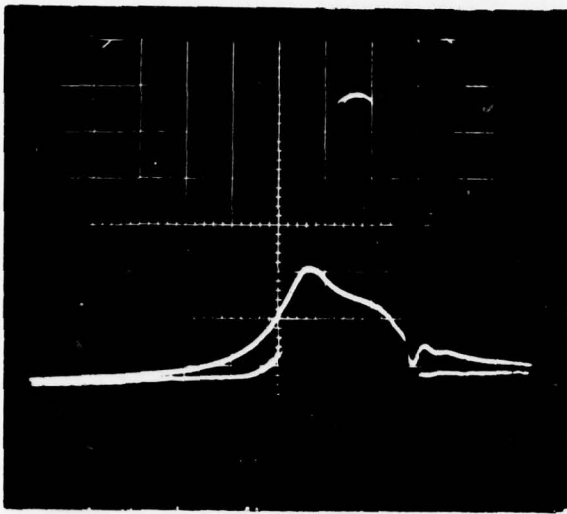


FIGURE 19. EFFECT OF SPEED ON "PURE" ROLLING TEMPERATURE RISE

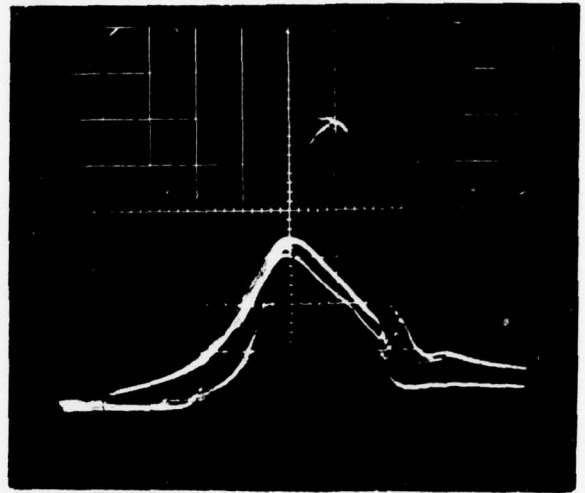
inlet temperature rise. The temperature drops roughly as the square root of the speed.

Load Effects

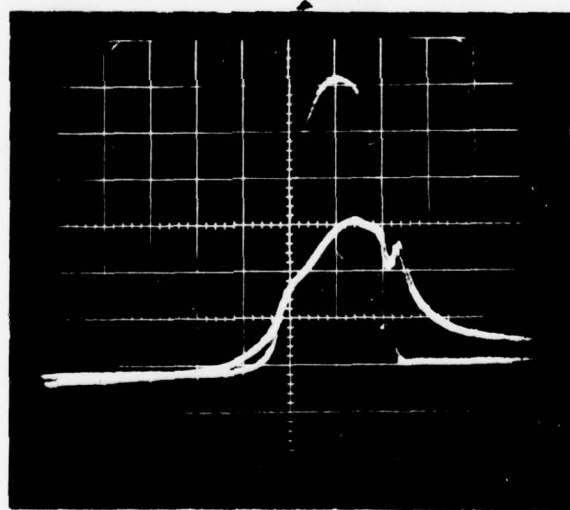
Figure 20 presents temperature-pressure traces for a load of 1.1 GPa. For this load, the temperature appears to rise to about 50 C under pure rolling for most of the lubricants, as opposed to 30 C for the .7 GPa load. It is possible that this load effect on temperature could, at least, partially explain anomolous load effect on EHD film thickness seen in various experiments such as BCL-X-ray experiments.⁽⁴⁾



(a) MIL-L-23699



(b) XRM-109



(c) Traction Fluid

FIGURE 20. TEMPERATURE-PRESSURE DATA FOR FOUR SELECTED LUBRICANTS

Speed = 2800 rpm (.076 m disks)
 Temperature Calibration = 16 C/div
 Load = 1.1 GPa
 Scope Sweep = 20 μ s/div

THEORETICAL EVALUATIONS

The purpose of the analyses has been to understand the nature of the EHD temperature and to assess the validity of the temperature measurements. As shown in the experimental section, these measurements have indicated that very high temperature rises can occur under pure rolling as well as rolling/sliding EHD contacts. Temperature rises on the order of 30-150 C can have a profound effect as lubricant rheology and, hence, on tractions and EHD film thickness.

Rheology Evaluations for Tractions

Very recently, rheology has been the topic of various researchers, including Johnson⁽⁵⁾, Winer⁽⁶⁾, Miller⁽⁷⁾, and Montrose⁽⁸⁾. As a result of the research by these scientists, very interesting non-Newtonian, limiting shear, transition, time transient, and viscoelastic effects have been isolated. The purpose of the BCL study has been to establish baseline data to be used to assess the effect of temperature on lubricant behavior. More work is needed in the area of interrelating these rheology analyses with thermal effects.

Under low slip conditions, shear heating due to slip should not be a major factor in controlling EHD tractions. By analyzing the slope of the traction-slip curves at zero slip, then, it should be possible to determine a pseudo-viscosity for the lubricant under rolling conditions. This viscosity is, of course, related to the inlet temperature rise and could be related to, say, glass-transition effects. For these evaluations, we have chosen to simply label this as a limiting viscosity for specific operating conditions.

To calculate this limiting viscosity, it is helpful to assume that the tractive force, F_T , between the disk can be expressed

$$F_T = \int_A \tau dA = \int_A \mu(P) \frac{\Delta V}{h} . \quad (1)$$

Here τ is shear stress, A is contact area, ΔV is slip, h is the EHD film thickness, and $\mu(P)$ is the viscosity of the lubricant at the contact pressure conditions. If μ is assumed to be a limiting viscosity, then

$$\mu = \frac{F_T h}{A \Delta V}, \quad (2)$$

where, for elliptical contacts,

$$A = \pi ab. \quad (3)$$

Here, b and a are the major and minor axes of the Hertz contact ellipse. Values of μ , as computed using Equation (2) are given in Table 1. The film thickness was computed using a semiempirical equation developed at BCL. ⁽⁴⁾

Temperature Rise Due to Sliding

In the first summary report, a theoretical analysis of the temperature rise due to slip was developed (see Appendix A). This analysis was based on heat generation due to slip (only) and heat loss due to conduction across the lubricant film. The temperature rise (T) could be written in the form

$$T = 3.1 \sqrt{\frac{K_L \mu(p) a}{K_S \delta V \rho c}} \frac{\Delta V}{h}, \quad (4)$$

where K_L and K_S are the lubricant and steel conductivity, δ is the temperature coefficient of viscosity, ρ is the density of the disk, c is the specific heat of the disk, V is the surface velocity, a is the half width of contact, and h is film thickness. Reasonable values for these parameters are

$$K_L = .30 \text{ N/sec C}$$

$$K_S = 35 \text{ N/sec C}$$

$$\delta = .03/\text{C}$$

$$V = 11 \text{ m/sec}$$

$$\rho c = 3.5 \times 10^6 \text{ N/m}^2\text{C}$$

$$a = 230 \text{ } \mu\text{m}.$$

Then,

$$T = 4.0 \times 10^{-6} \sqrt{\mu} \frac{\Delta V}{h} \frac{M^2 \text{sec}}{N}^{1/2} C . \quad (5)$$

Equation (5) can be used to compute the temperature rise due to sliding contact. The results of these estimates are summarized in Table 3 in comparison with the data taken from Figure 17. As can be observed, good agreement exists between theory and experiment.

Temperature Rise Due to Rolling

The energy equation of the lubricant film can be written⁽⁹⁾

$$\rho_L c_L V \frac{\partial T}{\partial x} - K_L \frac{\partial^2 T}{\partial y^2} = Q_s + Q_c \quad (6)$$

where ρ_L and c_L are the density and specific heat of the lubricant, K_L is the thermal conductivity, x is the tangential coordinate, y is normal coordinate, V is velocity, Q_s is the heating due to shear, and Q_c is the heating due to compression.

It is helpful to scale the left side of the equation in the following way:

$$\frac{\rho_L c_L V T_o}{a} \frac{\partial \bar{T}}{\partial \xi} - \frac{K_L T_o}{h_o^2} \frac{\partial^2 \bar{T}}{\partial \eta^2} = Q_s + Q_c . \quad (7)$$

Typical values for the constants are as follows:

$$\rho_L c_L = 1.5 \times 10^6 \text{ N/m}^2 \text{C}$$

$$a = 230 \text{ } \mu\text{m}$$

$$V = 11 \text{ m/sec}$$

$$K_L = .3 \text{ N/sec C}$$

$$h = 5 \text{ } \mu\text{m (max) .}$$

TABLE 3. ESTIMATE OF SURFACE TEMPERATURE RISE DUE TO SLIDING

Lubricant	Viscosity at Pressure		Film Thickness, 10^{-6} m	Temperature Rise C at 20% Slip	
	$\frac{\text{N Sec}}{\text{m}^2}$	Cp		Calculated	Measured
MIL-L-23699	16	$.16 \times 10^5$	1.35	27	30
XRM 109	100	1.0×10^5	5.1	18	25
Traction Fluid	320	3.2×10^5	1.46	108	130
Polyphenyl Ether	2330	23×10^5	4.7	90	75

Using these values then,

$$7 \times 10^{10} T_o \frac{\delta \bar{T}}{\delta \xi} - 1.2 \times 10^{10} T_o \frac{\partial^2 T}{\partial \eta^2} = Q_s + Q_c . \quad (8)$$

In the inlet zone (where $h > h_o$) for at least two of the lubricants evaluated, an approximation to Equation (5) can be written

$$\rho c V \frac{\partial T}{\partial x} \approx Q_s + Q_c . \quad (9)$$

Now, it can be shown that

$$\tau = \frac{\partial p}{\partial x} y \text{ (pure rolling equilibrium)} \quad (10)$$

$$\frac{dp}{dx} = 12 \mu(p) u \frac{h-h_o}{h^3} \text{ (Reynolds equation)} \quad (11)$$

$$Q_s = \frac{\tau^2}{\mu} \text{ (shear heating)} \quad (12)$$

$$Q_c = V B T_A \frac{dp}{dx} \text{ (Burton's }^{(10)} \text{ equation)} \quad (13)$$

$$h = h_o + \frac{a^2}{2R} \left[\xi \sqrt{\xi^2 - 1} + \ln (\xi + \sqrt{\xi^2 - 1}) \right] \quad (14)$$

(Hertz inlet shape)

Here,

p = pressure

h = film thickness at any point in the inlet region

τ = shear stress in the lubricant film

B = a compressibility constant

T_a = absolute temperature ($B T_A \approx .1$)

a = half-width of constant

$\xi = x/a$

R = the relative radius of the disk $\left(\frac{1}{R} = \frac{1}{R_1} + \frac{1}{R_2} \right)$

μ = viscosity of the lubricant [$\mu = \mu_o \exp(\gamma p - \delta T)$].

Equations (9) through (14) can be combined to the following form:

$$\frac{\partial \psi}{\partial \xi} = \frac{9\mu_o V\delta (h-h_o)^2}{\phi \rho_L c_L h^4} + \frac{12 \mu_o V B T_A \delta (h-h_o)}{\phi \rho_L c_L h^3} \quad (15)$$

and

$$\frac{\partial \phi}{\partial \xi} = - \frac{12\mu V \gamma}{\psi} \frac{h-h_o}{h^3} \quad (16)$$

where

$$\phi = e^{-\gamma p} \text{ and } \psi = e^{\delta T} . \quad (17)$$

Equations (14) and 15) are amenable to solution by numerical integration such as a Runge Kutta scheme.

Temperature predictions using Equation (14) through (16) are shown in Figure 21. Except for the MIL-L-23699 evaluation, an instability in the temperature solutions occurred as a result of very large pressure build-up. The unfortunate aspect of the equations are that they represent only the inlet region and do not merge easily with contact zone equations. The difficulty is that the pressure tends to infinite which in reality would deflect the surface and abate the pressure. The magnitudes of the temperature predictions in Figure (21) are higher than measured since the equations represent essentially an upper bound for temperature. However, the magnitudes of the predicted temperatures illustrate that the experimental data are reasonable and that very high temperatures occur in EHD contacts.

In the contact region, compressive heating is the major heat source under pure rolling conditions. If we ignore the shear stress effect in Equation (5), then it can be seen that

$$T = \frac{B T_A}{\rho_L c_L} p .$$

If, for example, $B T_A = .1$ and $p = .7 \times 10^9 \text{ N/m}^2$ (.7 GPa), then, $T = 46\text{C}$ which would be the adiabatic temperature rise due to compression in the contact region. This estimate further illustrates that the measured temperatures were reasonable.

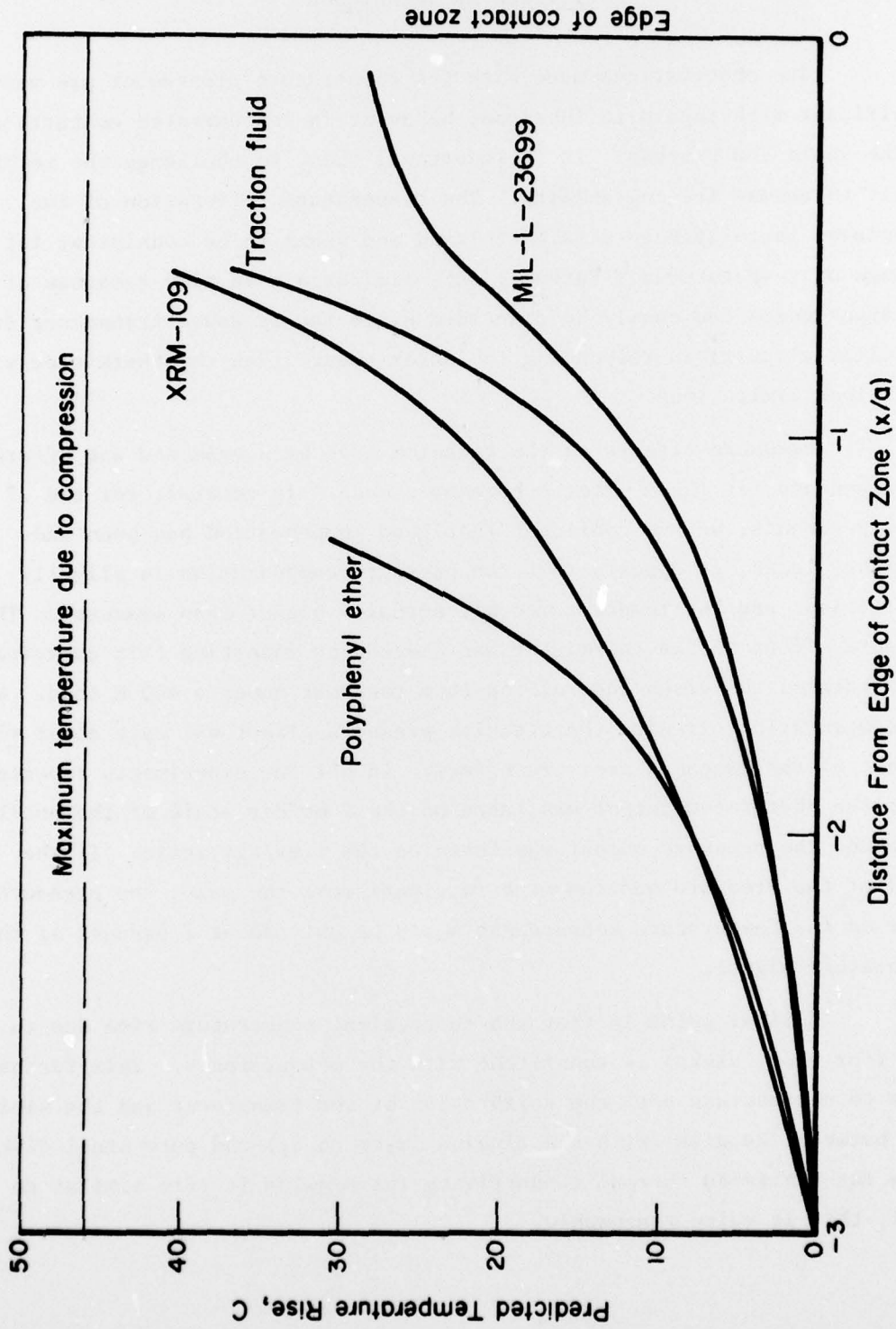


FIGURE 21. PREDICTED INLET ZONE TEMPERATURE

Critique of Techniques

The observations made with the temperature transducer are very significant with regard to lubricant behavior in concentrated contacts and on the whole EHD process. It is important, then, to challenge the technique itself to assess its reliability. The temperature calibration of the transducer is relatively straightforward and seems to be consistent for a range of temperatures. Further, such limitations as time response of the transducers can easily be discarded since the pressure transducer (with a similar circuit) is responding to faster events than the thermistor with no obvious limitations.

Pressure effects on the titanium have been examined and efforts to compensate for these effects have been made. In general, for the .7 GPa experiments, we are confident that good compensation has been made. At higher loads, it appears that the pressure compensation is slightly insufficient and the temperatures are actually higher than measured. The pressure effect on the thermistor was checked by inserting thin capacitance paper between the disks and rolling them together under a 400 N load. With the compensating circuit, the titanium pressure effect was only about ± 15 percent of the manganin pressure effect. In all the experiments reported here, the thermistor output was taken on the 2 mv/div scale of the oscilloscope and the pressure output was taken on the 1 mv/div scale. If the level of the pressure and temperature signal were the same, the pressure error on the temperature measurement would be only about 7 percent of the temperature signal.

A final point is that the theoretical temperature rise due to slip (for steel disks) is consistent with the measurements. This further tends to corroborate both the calibration of the transducer and the similitude between the disk (with the alumina layer on it) and pure steel disks. Since the published thermal conductivity for alumina is very similar to steel, this is quite reasonable.

CONCLUSIONS

The objective of the project has been to evaluate the role of temperature in the EHD process. Based on the project experiments, the following conclusions were made.

- (1) The inlet temperature rise was approximately 30 C for all four lubricants evaluated at .7 GPa.
- (2) The temperature drop in the contact region (under pure rolling conditions) depends heavily on the lubricant and apparently the lubricant film thickness (i.e., the volume of heated fluid).
- (3) The temperature rise under pure rolling varies roughly as the square root of rolling speed and increases with increasing load.
- (4) Contact zone temperatures as high as 200 C have been measured under high slip conditions with a traction fluid.

Analyses in connection with the experiments indicate that

- (1) The pure-rolling temperature rise can be explained based on inlet shear and compression heating.
- (2) The measured temperature rise due to slip is reasonable and consistent. Further, this temperature rise could be used to explain much (and, perhaps all) of the drop off in traction due to slip, especially for thick film lubrication.
- (3) The observed drop off in temperature with decreasing speed makes the results reasonable in comparison with other researchers.
- (4) The increase in temperature with increasing load hints that temperature is a major reason for anomalous decreasing film thickness with load, as observed with X-ray measurements.

- (5) The overall magnitude of the temperature measurement makes isothermal EHD film thickness theories very suspect for real bearing contacts

The results of this project point to several areas where more research would be fruitful. These areas include

- (1) An analysis of the temperature rise in pure rolling for a range of loads and speeds to evaluate
 - (a) Effect of load/temperature on film thickness
 - (b) Effect of speed/temperature of film thickness.
- (2) Experiments to determine the effect of non-Newtonian lubricants such as polymer thickened oils or greases on contact zone temperatures and bearing-gear performance.
- (3) A better definition (both analytical and experimental) of the role of temperature in traction to aid in designing traction drive units.

REFERENCES

- (1) Kannel, J. W. and Bupara, S. S., "Rheology of Lubricant in Real Bearing Contacts", Trans ASME, Vol. 97 Ser F No. 3, April, 1975, pp 228-235.
- (2) Kannel, J. W. and Zugaro, F. F., "The Role of Temperature in EHD", ONR Progress Report, October, 1976.
- (3) Kannel, J. W., Zugaro, F. F., and Dow, T. A., "A Method for Measuring Surface Temperature Between Rolling/Sliding Steel Cylinders", ASME paper No. 77-Lub-1, presented at ASME-ASLE Conference, Kansas City, Missouri.
- (4) Bell, J. C. and Kannel, J. W., "Interpretation of the Thickness of Lubricant Films in Rolling Contact 2, Influence of Possible Rheological Factors", Trans ASME Vol. 93, Series F, No. 4, October, 1971, pp 485-497.
- (5) Johnson, K. L. and Teuhaarwerk, "Shear Behavior of Elastohydrodynamic Oil Films", Proc. R. Society London A, 356, 1977, pp 215-236.
- (6) Alsaad, M., Bais, S., Sanborn, D. M. and Winer, W. O., "Glass Transition in Lubricants: Its Relation to Elastohydrodynamic Lubrication", (EHD) School of Mechanical Engineering, Georgia Institute of Technology report, April, 1977.
- (7) Miller, R. S., "On the Mechanical Behavior of Entrance Materials in Concentrated Contacts", Trans ASLE, Vol. 19, pp 1-16.
- (8) Montrose, C. J., Moynihan, C. T. and Sasabe, H., "Dynamic Shear and Structural Viscoelasticity in Elastohydrodynamic Lubrication", Catholic University report to ONR.
- (9) Bell, J. C., Kannel, J. W., and Allen, C. M., "The Rheological Behavior of a Lubricant in the Contact Zone of a Rolling-Contact System", Trans ASME J. of Basic Eng., Vol. 68, Series D, No. 3, Sept, 1964, pp 423-435.
- (10) Burton, R. A., Discussion to Reference (9) above.
- (11) Kannel, J. W. and Bell, J. C., "A Method for Estimation of Temperature in Lubricated Rolling-Sliding Gear on Bearing Elastohydrodynamic Contacts", Proc., I. Mech E. Engr. EHD Symposium, London, 1972, pp 118-130.
- (12) Kannel, J. W. and Walowit, J. A., "Simplified Analysis for Traction Between Rolling-Sliding Elastohydrodynamic Contacts", ASME Trans. Vol. 93, Series F, No. 1, January, 1971, pp 39-44.
- (13) Cheng, H. S., "A Refined Solution to the Thermal Elastohydrodynamic Lubrication of Rolling and Sliding Cylinders", Trans, ASLE, Vol. 8, No. 4, October, 1965, pp 397-410.

APPENDIX

ESTIMATION OF SURFACE TEMPERATURE
RISE DURING ROLLING/SLIDING CONTACT

APPENDIX

ESTIMATION OF SURFACE TEMPERATURE RISE DURING ROLLING/SLIDING CONTACT

Energy Equation for the Lubricant Film

The purpose of this analysis is to develop a simple method for estimating surface temperature rise due to EHD tractions. The approach presented here is similar to the one developed by Kannel and Bell.⁽¹¹⁾ However, in that paper, a lubricant model using an exponential temperature relationship was used. This model resulted in an overly complicated expression for surface temperature distribution. A more convenient lubricant model is of the form

$$\mu = \frac{\mu_1 \exp(\gamma p)}{1 + 8(T - T_1)} \quad (A-1)$$

where

μ = the lubricant viscosity

μ_1 = viscosity in the inlet region

γ = pressure viscosity exponent

p = pressure

δ = temperature coefficient of viscosity

T = temperature

T_1 = inlet zone temperature .

Ignoring convection of heat along the film in favor of conduction across the film, the energy equation for a Newtonian lubricant model can be written⁽¹²⁾

$$K_L \frac{\partial^2 T}{\partial y^2} + \left(\mu \frac{\partial u}{\partial y} \right)^2 = 0 \quad (A-2)$$

where,

T = temperature

K_L = thermal conductivity of lubricant.

It is helpful (though not mandatory) to assume that the temperature distribution in the lubricant film is symmetrical about the centerline. Also, it is assumed⁽¹²⁾ that the shear stress is constant across the film. With these assumptions and the definition of a thermal loading parameter, T_L , given by

$$T_L = (u_2 - u_1) \sqrt{\frac{u_1 \delta}{K_L}}, \quad (\text{A-3})$$

there results from Equation (A-2)

$$\left. \frac{\partial T}{\partial y} \right|_s = \frac{T_L}{h\delta} \exp \frac{\gamma p}{2} \operatorname{arccot} \left[\frac{2(1 + \delta T[0])}{T_L \exp(\gamma p/2)} \right], \quad (\text{A-4})$$

or

$$\left. \frac{\partial T}{\partial y} \right|_s \approx \frac{\pi T_L}{2h\delta} \exp \frac{\gamma p}{2}. \quad (\text{A-5})$$

Here,

$u_2 - u_1$ = sliding velocity

h = film thickness

K_L = thermal conductivity of lubricant

s = surface temperature or temperature gradient.

Heat Transfer to the Solid

Using the equation of Cheng⁽¹³⁾, the heat transfer to the solid can be written

$$T_s - T_i = \frac{K_L}{\sqrt{\pi \rho c u_1 k_s}} \int_{-a}^x \left. \frac{\partial T}{\partial y} \right|_s \frac{d\xi}{\sqrt{x - \xi}} \quad (\text{A-6})$$

Combining (A-5) and (A-6), the following expression for surface temperature results:

$$T_s - T_i = \frac{1}{2\delta h} \sqrt{\frac{\pi k_s}{u_1}} \frac{K_L}{K_s} \frac{x}{-a} \exp\left(\frac{\gamma P(\xi)}{2}\right) \frac{d\xi}{\sqrt{x-\xi}}, \quad (\text{A-7})$$

where,

k_s = diffusivity of steel

K_s = thermal conductivity of steel

ρ = density of the lubricant

c = specific heat

a = half-width of the contact region

T_i = inlet temperature .

Approximate Solution for Surface Temperature

The pressure distribution between heavily loaded EHD contacts can be approximated to a high degree of accuracy by the equation

$$p = p_h \sqrt{1 - \left(\frac{x}{a}\right)^2}. \quad (\text{A-8})$$

If we assume that heating occurs very near the center of contact, then,

$$\exp\left\{\frac{\gamma P_h}{2} \sqrt{1 - \frac{x^2}{a^2}}\right\} \approx \exp\frac{\gamma P_h}{2} \exp\left[-\frac{1}{2} \frac{\gamma P_h}{2} \left(\frac{x}{a}\right)^2\right]. \quad (\text{A-9})$$

Now, by defining

$$\phi = \left(\frac{\gamma P_h}{2}\right)^{1/4} \left(\frac{x}{a} - \frac{\xi}{a}\right)^{1/2}, \quad \text{and } \beta = \frac{x}{a} \left(\frac{\gamma P_h}{2}\right)^{1/2}, \quad (\text{A-10})$$

there results

$$T_s - T_i = \frac{T_L}{\delta h} \frac{K_L}{K_s} \sqrt{\frac{\pi k_s a}{u_1}} \left(\frac{2}{\gamma P_h}\right)^{1/4} \exp\left(\frac{\gamma P_h}{2}\right) f(\beta), \quad (\text{A-11})$$

where,

$$f(\beta) = \int_0^{\infty} \exp\left[-\frac{1}{2}(\beta - \phi^2)^2\right] d\phi. \quad (\text{A-12})$$

Values of $f(\beta)$ are presented in Figure A-1. The peak value is 1.3. Combining Equation A-3 and A-11, there results

$$T_{s_{\max}} = 2.1 \sqrt{\frac{K_L}{K_S} \mu_o \frac{e^{\gamma p_h a}}{\delta V \rho c} \frac{\Delta V}{h} \left(\frac{2}{\gamma p_h}\right)^{1/4}} \quad (A-13)$$

For an elliptical contact region, it can be shown that

$$\mu_{\text{ave}} = \frac{1}{A} \int_A \mu(p) \, dA, \quad (A-14)$$

or*

$$\mu_{\text{ave}} = \frac{1}{ab} \int_0^{p_h} \mu_o e^{\gamma p} (-2\pi ab \, p \, dp) \quad (A-15)$$

Thus, (approximately)

$$\mu_o e^{\gamma p_h} \approx \mu_{\text{ave}} \frac{(\gamma p_h)^2}{2(\gamma p_h - 1)}, \quad (A-16)$$

if we assume that $\gamma p_h \approx 3$ for high pressure condition. Then,

$$\mu_o e^{\gamma p_h} = 2.25 \mu_{\text{ave}}, \quad (A-17)$$

and Equation (A-13) becomes

$$T_{s_{\max}} = 3.1 \sqrt{\frac{K_L}{K_S} \frac{\mu_{\text{ave}} a}{\delta V \rho c} \frac{\Delta V}{h}} \quad (A-18)$$

* See Reference (1), Equation (21).

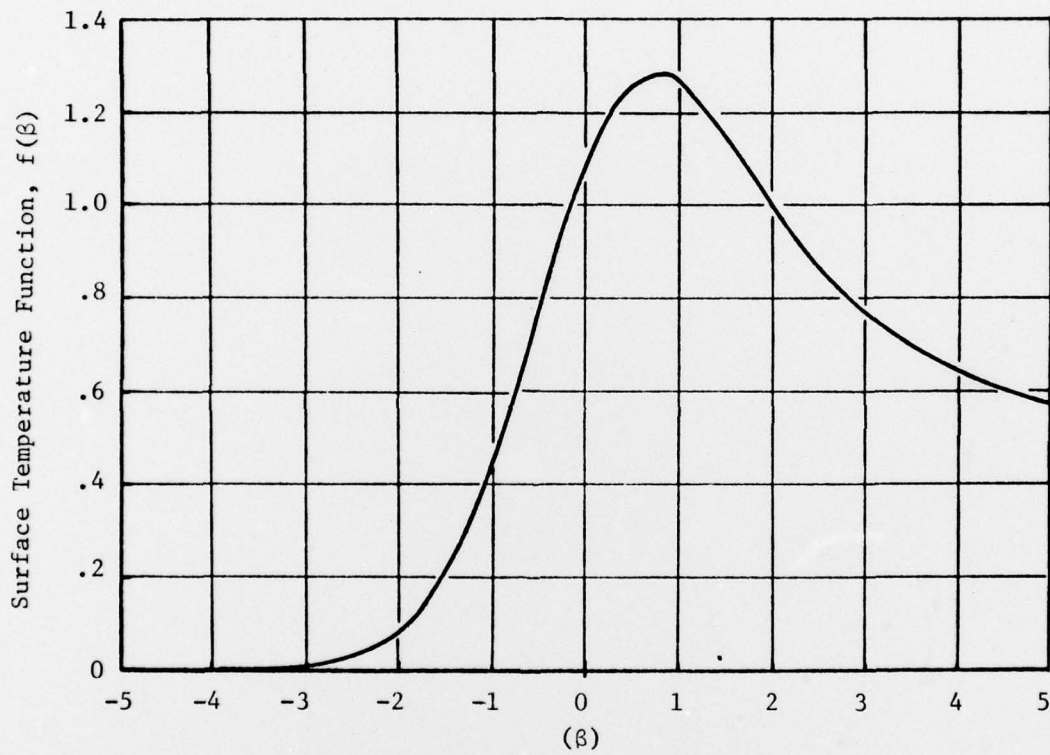


FIGURE A-1. SURFACE-TEMPERATURE FUNCTION VERSUS DIMENSIONLESS POSITION IN CONTACT ZONE